Results of on-site monitoring campaign and parametric laboratory testing

GEOTHERM – Geothermal energy from sedimentary reservoirs
– Removing obstacles for large scale utilization
Innovation Fund Denmark: project 6154-00011B
(Report M5.4 in WP5)

Troels Mathiesen, Jakob Mølholm og Johan Braüner Nielsen
Brøndby, 16 December 2019

FORCE Technology Norway AS
Nye Vakås vei 32
1395 Hvalstad, Norway
Tel. +47 64 00 35 00
Fax +47 64 00 35 01
info@forcetechnology.no
www.forcetechnology.no

FORCE Technology, Mail Office
Park Allé 345
2605 Brøndby, Denmark
Tel. +45 43 26 70 00
Fax +45 43 26 70 11
force@force.dk
www.forcetechnology.com

Contents

Executive summary

This report concludes the tests made in Work Package 5 (WP5) in the Geotherm project with the objective of addressing the problems of injectivity in the Danish geothermal plants. In order test on-site while the plants were running, a customised rig/equipment was constructed. The design of the equipment enabled corrosion measurement and automated water sampling, measuring pH, dissolved oxygen (DO) and oxidation-reduction potential (ORP). The measurements included all Danish plants, i.e. Margretheholm, Sønderborg and Thisted. In parallel to this, parametric tests were performed in the laboratory with focus on effects of residual oxygen, temperature, lead deposition and corrosion inhibitor dosage. A pre-study formed the basis for the entire testing campaign, which aimed at understanding any interaction between brine and equipment that could cause particle release and possible plugging of the injection well. All available information on reduced injectivity was reviewed, including the reports prepared by the French, German and Swedish partners in the Geotherm project as well as reports about the Danish geothermal plants and scientific papers. Site visits were also part of the preparation and testing work. The most important results obtained from the testing campaign can be summarised as follows:

- Deposition of lead and galvanic corrosion of steel may contribute to the reduced injectivity at Margretheholm. The dosage of corrosion inhibitor has only limited effect as shown in the on-site measurements and laboratory testing.

- Quite high corrosion rate of steel is observed at the injection well in Sønderborg. Several independent test methods point to oxygen ingress as the main reason, but final confirmation by DO measurement is needed.

- Mill scale on the inside surface of well tubing may potentially release large amounts of rust flakes, plugging the well. Mill scale is extremely difficult to dissolve, making a well workover impossible. Apparently, the mill scale issue is not well recognised in the industry and standards.

- Requirements for well tubing for geothermal energy (where particle contamination is unacceptable) should be stricter than those met in the oil and gas industry.

- Measurements in Thisted has confirmed the absence of dissolved oxygen in the brine, thereby providing ideal conditions to control corrosion and avoid particle formation.

- The tolerance of stainless steel in the high-saline brine is very low, especially in hot brine. Stainless steel 316L is already used for small components in the plants today but upgrading pipe systems or well tubings is not yet recommendable, unless the efforts to control ingress of oxygen are intensified at the same time.

Dansk resumé

Denne rapport sammenfatter resultaterne af test, der er foretaget i Arbejdspakke 5 (WP5) i Geotherm-projektet med det formål at tackle problemer med nedsat injektivitet i danske geotermiske anlæg. Test i anlæggene, mens de var i drift, har omfattet design af specialudstyr dels til korrosionsmåling, dels til automatisk vandprøvetagning for måling af pH, opløst ilt (DO) og redoxpotential (ORP). Målingerne har omfattet alle danske anlæg, dvs. Margretheholm, Sønderborg og Thisted. Parallelt med dette er der gennemført parameterstudier i laboratoriet med fokus på at undersøge effekten af opløst ilt, temperatur, blyudfældning og korrosionsinhibitordosering. En forundersøgelse dannede grundlaget for hele testkampagnen, der sigter mod at forstå enhver interaktion mellem den saltholdige geotermiske vand og udstyret, dvs. processer, som kan frigøre partikler og medføre tilstopning af injektionsbrønden. Alle tilgængelige oplysninger blev gennemgået, inklusive rapporter udarbejdet af de franske, tyske og svenske partnere i Geotherm-projektet samt rapporter om de danske geotermiske anlæg samt videnskabelige artikler. Besøg på anlæggene udgjorde også en del af forberedelses- og testarbejdet. De vigtigste resultater, opnået i den samlede testkampagne, kan sammenfattes til følgende:

- Aflejring af bly og galvanisk korrosion af stål kan bidrage til den reducerede injektivitet i Margretheholm. Doseringen af korrosionsinhibitor har kun begrænset virkning, hvilket er vist i on-site målingerne og laboratorietest.

- Der observeres en forholdsvis høj korrosionshastighed af stål ved injektionsbrønden i Sønderborg. Tre uafhængige målemetoder peger på iltindtrængning som hovedårsagen, men endelig bekræftelse ved måling af opløst ilt afventes.

- Glødeskal på den indvendige side af brøndrør (dvs. foringsrør og borerør) kan frigive store mængder rustflager, som kan tilstoppe injektionsbrønden. Glødeskal er ekstremt vanskeligt at opløse, hvilket gør det umuligt at reetablere en brønd, som er tilstoppet pga. glødeskal. Brøndrør med glødeskal er et hidtil overset problem i geotermi-branchen og standarderne, som Geotherm-projektet har bragt i fokus.

- Kravene til brøndrør i geotermisk energi, hvor selv en minimal partikelforurening er uacceptabel, bør være strengere end de krav, der stilles i olie- og gasindustrien.

- Målinger i Thisted har bekræftet, at det geotermiske vand er iltfri, hvilket giver de ideelle betingelser for at kontrollere korrosion af stål og undgå partikeldannelse.

- Bestandigheden af rustfrit stål overfor geotermisk vand med højt saltindhold er meget lille, især i den varme vandstrøm fra produktionsbrønden. Rustfrit stål 316L bruges allerede til små komponenter i anlæggene i dag, men en opgradering af udstyr og brøndrør til rustfrit stål frarådes, medmindre bestræbelserne på at kontrollere indtrængen af ilt intensiveres på samme tid.

1 Introduction

Two out of three Danish geothermal plants are experiencing reduced injectivity in their injection wells. Several attempts have been made to understand and solve the problems. Corrosion, scaling or microbial growth are suspected as contributing elements, but the root cause has yet to be identified and it needs to be fully documented.

The objective of WP 5 in the Geotherm project has been to plan and conduct tests, addressing the problems of injectivity in the Danish geothermal plants. The current report summarises the results of this effort.

As stated in the application, the tests include on-site monitoring and parametric tests. To identify the most appropriate test methods, available information on the topic has been reviewed. This includes the reports prepared by the French, German and Swedish partners in the Geotherm project refs 1-3. Moreover, reports about the Danish geothermal plants and literature have been reviewed. This leads to the test plan (M5.2) that has been executed during the last two years.

The overall approach of our study can be described as:

1. Establish an understanding of Danish plants (design, materials, service history etc)
2. Review experience from European partners and literature about plants, similar to Danish plants
3. Identify hypothesis for reduced injectivity
4. Review experience from monitoring campaigns performed in geothermal plants, globally
5. Propose strategy for on-site monitoring and parametric testing
6. Perform testing

1.1 Key facts about Danish geothermal plants

The key facts for the Danish geothermal plants have been summarised in the table enclosed in Appendix A. The same information was requested as a basis for the reports, prepared by our European partners, refs 1-3.

The three Danish facilities are comparable with only minor differences in formation type, plant design and operation. However, the oldest plant in Thisted (THI) has had problems with slightly reduced injectivity over time, whereas Margretheholm (MAH) and Sønderborg (SFJV) are both experiencing considerably reduced injectivity. Several reports by experts review the problems, refs 4-20. Important observations have also been made at meetings and inspections during the start of Geotherm, ref 21.

The Danish plants use non-coated steel tubing for the wells (except for the most recent well in Thisted). A submersible pump in the production well feeds the surface installation with warm brine. The brine is filtered in bag filters in stainless steel or steel canisters before reaching the titanium plate heat exchangers (MAH and SFJV) or the absorption heat pump (THI). Compact cartridge filters remove particles before the brine is reinjected to the formation, using an injection pump. In one The brine solution is potentially very corrosive due to the high salt concentration (TDS 164-218 g/l, Na-Ca-Cl). However, strict precautions (such as nitrogen blanketing) are applied to avoid ingress of air/oxygen, thereby removing the driving force for corrosion.

As discussed later, the current understanding of the problems at Margretheholm involves lead deposition, whereas the problems in Sønderborg are possibly caused by air ingress and release of mill scale from the well tubing. Sulphide production due to microbial sulphate reduction, as indicated from preliminary tests, may also affect injectivity. However, other issues beyond this report are also suspected as a major cause of poor injection in Sønderborg, such as improper well completion and gravel pack.

1.2 Experiences from French, Swedish and German geothermal plants

In France, thirteen geothermal operations are comparable to Danish conditions. The review in ref 1 mentions that the operations frequently encountered problems with the reinjection of geothermal water, and only those using clay-sandstone reservoirs at modest depths (600 to 1200 m) were successful. Problems with mineral precipitation and scaling are common at geothermal plants, whereas corrosion seems to cause only minor problems, but in order to protect the installations, preventing corrosion is still important.

The experiences from the geothermal plant in Lund in Sweden are described in detail in ref 2. The observed problems with reinjection are caused by variations in the formation and well completions. However, regular airlifting and a water jetting operation of the wells have solved the problem. Corrosion and erosion have occurred in a submersible pump due to poor design in the production well, but this issue had no influence on reduced injectivity. Minor scaling has also been noted, but the mineralogy was not analysed since water jetting apparently solved the problem.

The experiences from operating geothermal plants for more than two decades in the northern part of Germany are summarised in ref 3. Five plants are reported and the configuration in two plants differs from that of the Danish plants, involving one borehole or reversible operation (both heating and cooling). In Germany, the tendency is to replace steel tubing with corrosion resistant materials, such as GRE or liners. However, the reported incidents of reduced injectivity are not related to corrosion, but rather high mineralisations, mobilisation of particles from the reservoir, precipitations, clogging of the pores, bacterial activity, clay swelling and technical inadequacy of the installations.

The reported causes of reduced injectivity in the three reports are summarised in Table 1. Neither of the plants are identical to the Danish plants, but the observations on lead precipitation and possibly bacterial growth may show resemblance with the issues observed in Denmark.

Table 1. Summary of experience on reduced injectivity in French, Swedish and German geothermal plants, refs 1-3.

Plant	Causes of reduced injectivity	Remarks
Melleray, FR	Destabilisation of formation	Iron Oxidising Bacteria (IOB) and Sulphate Reducing Bacteria (SRB) may affect corrosion and scaling, if plant becomes operational
Achères, FR	Inadequate filtering prior to injection Turbulence/erosion in well	Well tubing lined (no bare steel)
Cergy-Pontoise, FR	No problems reported	
Paris, FR	Air leaking into surface loop causing bubbles in reservoir	Solved by degassing system
Châteauroux, FR	No injection well, but problems in production well due to location	Solved by drilling new well and modifying strainer filters
Clermont-Ferrand, FR	Well collapsed during drilling	Project abandoned
Kronenburg, FR	Changes in reservoir (marked diagenisis)	
Plaisir and Thiverval-Grignon, FR	No problems reported, well works both ways at <40 m^3/h	Heat storage
Bordeaux, FR	No injection well	No reported problems, such as corrosion. Tubing is stainless steel.
Lund, S	Variations in formation and quality of well completion	Mitigated by regular airlifting (3-5 times/year) and hydro jetting of screens
Neustadt-Glewe, DE	Mineralisation due to degassing, PbS, FeS_2, $CaCO_3$, $BaSO_4$	Acid-soluble scale, 15 % HCl Well tubing lined (no bare steel) Sulphate Reducing Bacteria (SRB) and Methanogenic bacteria present but do not affect injectivity
Neubrandenburg, DE	Precipitation of lead and copper compounds when brine is cooled	Mitigated by regular soft acidizing. Two-way operation; cooling in summer and heating in winter. Sulphate-reducing microbes identified.
Waren/Müritz, DE	No problems reported	Plant modernisation involved change to corrosion resistant materials (GRP, polymers, titanium)
Nueruppin, DE	Borehole cementation problem	
Hannover, DE	Salt precipitation, halite (NaCl)	One borehole – two reservoirs

1.3 Known mechanisms for reduced injectivity

The literature survey has included a brief review of approx. 80 international papers on geothermal energy and corrosion. Most of the papers concern geothermal sites operating under conditions far from those found in the Danish plants, i.e. higher temperatures, steam production and other formation types. The plants resembling the Danish plants are to a great extent already covered by the French, Swedish and German partners (refs 1-3). In addition to this, knowledge can be obtained from the plants in Poland and Netherlands.

On this basis, the main mechanisms for obstructing reinjection are listed below:

- Reservoir rock susceptible to diagenesis (fines migration)
- Well completion quality (location, design, gravel configuration)
- Inadequate filtering prior to injection
- Precipitation of salts due to cooling or air ingress in surface plant
- Degassing of CO_2, pH increase, scaling
- Oil residues becoming viscous in injector well
- Improper flow in well (turbulence, erosion and gas bubbles)
- Bacteria facilitating precipitation of minerals

Corrosion has not been reported as a problem causing reduced injectivity, although this degradation mechanism still deserves high attention to preserve the integrity of the installations.

Operational issues in geothermal energy across the entire Europe have been summarised in the so-called "Magna Carta", ref 22. This diagram can suggest methods for problem solving when the cause of reduced injectivity has been identified.

1.4 Initial hypothesis

Based on the above data from the Danish plants and the international partners, the initial understanding of the problems with reduced injectivity has been summarised as follows.

Margretheholm
Measurements in 2006 have shown quite high corrosion rates of carbon steel (0.3 mm/year), especially when galvanically connected with stainless steel (>1 mm/year). Moreover, penetrating corrosion has been observed in local areas under influence of high flow. According to expert evaluations, the observed corrosion in the surface plant is caused by galvanic deposition of lead. Lead deposits have also been identified in the injection well. Consequently, tests have been initiated to prevent corrosion and lead deposition by injecting a film-forming corrosion inhibitor. No information has been available about the surface condition of the installed well tubing (i.e. whether mill scale was removed).

Deposition of lead as pure metallic lead or sulphides has also been observed in plants in Germany and the Netherlands. However, it is not clear whether the injectivity was affected by this but scaling inside the installations has been observed, ref 20.

It is necessary to understand and control the deposition of lead in order to minimise both corrosion and accumulation of Naturally Occurring Radioactive Material (NORM). Most likely, this effort will also improve injectivity.

Sønderborg

Several expert evaluations were available at the project start. Relatively high iron sulphide levels in produced water after standstill periods indicate sulphide production by microbes. Bottom-hole sampling has shown the presence of mostly iron oxides that are impossible to dissolve in soft acids (1 % HCl and 1 % HNO_3) as well as stronger acids (5 % HCl and 2 % HF). Such deposits have also been identified as mill scale in surplus tubing located at the plant.

IFE has estimated a corrosion rate of 0.2–0.6 mm/year driven by the dissolved CO_2-gas. However, corrosion matching this figure has not been observed in the plant, ref 6.

On this basis, the main hypothesis for reduced injectivity aims at the release of mill scale from injection well casing, Figure 1. Any corrosion taking place in the system may possibly promote the release of mill scale. The mechanisms considered here include, at different locations in the plant, air ingress, bacteria (SRBs) and CO_2-corrosion.

Figure 1. Mill scale in new tubing at Sønderborg.

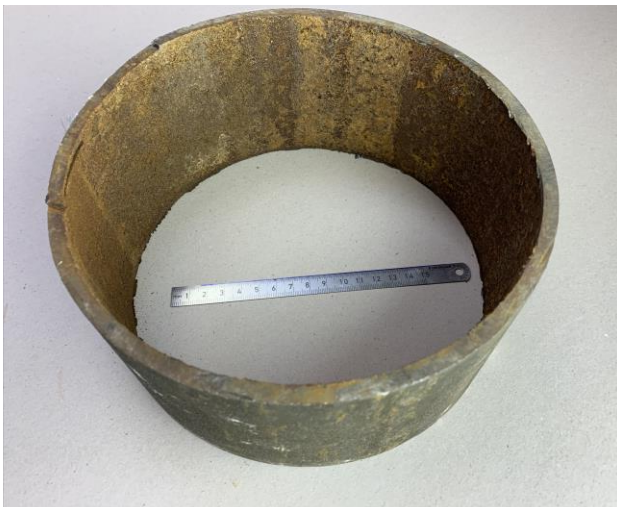

Figure 2. Pipe section from Thisted showing only superficial corrosion after 30 years' service.

Thisted

The plant shows the expected and slow increase of pressure in the TH-3 injection well after 30 years' operation. We are not aware of any problems with corrosion of the steel tubing, which has been confirmed by examination of a pipe sample, Figure 2. Because of the successful operation, there has been no need for sampling, investigations or expert evaluations. In order to ensure clean operation, injection is conducted via a 7-inch sandblasted tubing inside the well casing. This may very well be the reason why Thisted is not experiencing the same problems as Sønderborg, where such measures have not been taken. In comparison, the strainer in Thisted is also wider, 0.3 mm as opposed to 0.15 mm at Sønderborg, thereby minimising the risk of clogging.

1.5 Test plan

Attempts had already been made to monitor corrosion and scaling at both Margretheholm and Sønderborg at the start of the project. Based on this and the above, a refined strategy was established for the testing campaign as described below. In some cases, the original test plan had to be adjusted due to operational problems in the geothermal plants.

Margretheholm

A side stream unit measuring corrosion in the low-pressure section after the bag filters had been installed by Nalco to verify the effect of inhibitor dosage. The unit measures:

- Corrosion rate (using linear polarisation resistance measurement, LPR)
- Oxidation reduction potential (ORP)
- Temperature
- pH
- Corrosion coupons (showing corrosion type, weight loss and scaling)

This unit has been used in the project for a short period. Additionally, it was planned to add a unit that could be installed in the high-pressure section after the injection pump. However, due to the operational problems at Margretheholm in 2018-2019, it was not possible to carry out such testing.

Sønderborg

A side stream unit measuring corrosion in the high-pressure section after the injection pump had been installed in the start of the project. The unit measures:

- Galvanic corrosion current between brass and steel
- Corrosion rate using electrical resistance probe (ER)
- Corrosion coupons (showing corrosion type, weight loss and scaling)

The first measurement campaign with the side-stream unit was performed from February 2017 to May 2017, exposing coupons only. The second from November 2017 to April 2018. The third campaign started in October 2018 and ended in December 2018.

The rack for measuring pH, dissolved oxygen (DO) and oxygen reduction potential (ORP) was built by Emerson and ready for installation in the autumn of 2018. The rack intended for Margretheholm was shipped to Sønderborg for installation, as Margretheholm was out of service.

The two racks were installed and up and running on 13 December 2018; one on the high-pressure side after the injection pump, and the other on the low-pressure side after the filters.

Due to unforeseen injectivity problems, the Sønderborg plant was shut down on 20 December 2018. The issues proved unsolvable in the short term, so the measurements were not re-started.

Thisted

Originally, no testing was planned in Thisted due to the absence of problems in this plant. But since the water sampling racks from Margretheholm and Sønderborg were available, it was decided to perform measurements to gain experience with equipment and obtain information about the water chemistry in Thisted. The measurement took place in April 2019.

Continuous water sampling

The above-mentioned configuration did not measure dissolved gases (e.g. CO_2, H_2S), dissolved solids (TDS), changes in composition or the presence of bacteria. Such information was obtained from the water samples taken as part of WP3 (except bacterial analysis), Appendix B. Since the expected changes are very small, regular sampling will suffice for interpretation of corrosion and scaling.

Microbiological analysis of water samples may be relevant at a later stage if the corrosion probes contain scaling that may originate from bacterial growth. At present, microbial growth is not considered a prime cause of reduced injectivity in the Danish plants. This is supported by the results from the European partners in Table 1.

Testing in lab – parametric studies

The conditions in the geothermal plants have been simulated in the laboratory to study the effects of operational parameters, affecting corrosion or scaling. The tests were performed in autoclaves in brine samples from Margretheholm. Electrochemical techniques were applied to obtain a rapid response. The test plan has included evaluation of the items listed below:

- Effect of minute ingress of oxygen
- Effects of temperature and flow
- Establishment of a new electrochemical cell to measure galvanic effects of lead
- Effect of lead: Examine effect on galvanic corrosion by adding small amounts of dissolved lead
- Corrosion inhibitor: Evaluate performance on lead corrosion

Additional testing has included microscopy and verification of methods for dissolving the particles, found in the plants, especially mill scale.

2 Results of on-site visits and monitoring

2.1 Site visits

Prior to the on-site testing, each plant was visited at least once to review service history and to plan the tests. Some observations were made during these visits.

Margretheholm

Visual inspection of open pipework in September 2016 revealed dark grey deposits, later confirmed to consist primarily of metallic lead, Figure 3. Such dark grey deposits were present in nearly all the inspected pipes.

During the visits, we were told that one incident of penetrating corrosion had occurred in the plant. The leak was found in an elbow just after the heat exchanger. No photos are available, but the cause of the leak was presumed to be internal corrosion caused by lead deposits in conjunction with turbulent flow in connection with the elbow. This mechanism has previously been described by Schröder ref 23, Figure 4. A report by GEUS in 2015 also suggests this mechanism, ref 24-27. It includes a detailed analysis of the distribution of lead deposits, throughout the Margretheholm plant. The deposition of lead is not uniform and looks like Figure 4 in many areas. The highest amount of lead deposits was seen in the production well and flowlines to the surface plant, whereas the injection well showed only few lead deposits.

Figure 3. Lead deposits inside piping at production well at Margretheholm.

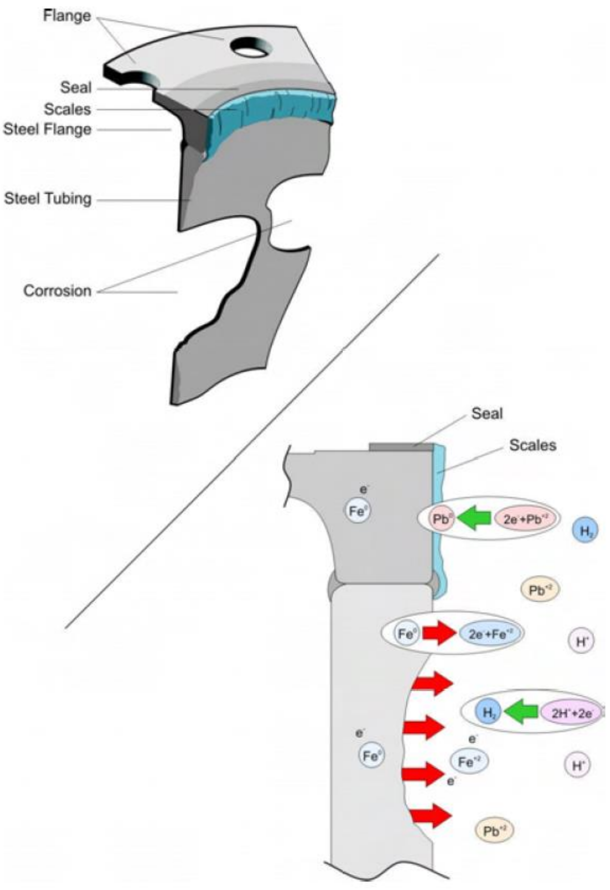

Figure 4. Electrochemical corrosion of iron due to deposition of lead, ref 23.

Sønderborg

The geothermal plant in Sønderborg was visited several times in 2016, 2017 and 2018. No corrosion was observed apart from what appeared to be superficial internal rust on some of the pipes leading to the injection well.

Tubing identical to what had been used originally was lying outside the plant, sealed with plastic end caps. These were opened and a visual inspection revealed significant amounts of what appeared to be rust flakes from mill scale, Figure 1.

Filter housing made from stainless steel AISI 316 with 2 microns filter bags were equipped with carbon steel anodes, Figure 5. The anode was depleted after roughly 6 months, the consumption indicating oxygen ingress beyond what could be expected from changing the filters alone.

Thisted

No observations of corrosion were made. A section from a 30-year-old pipe that had been made redundant from the latest injection well commissioning was available for inspection. No discernible loss of wall thickness was visible apart from light superficial corrosion, likely caused by water remnants on the surface after being cut out, Figure 2.

The new injection well (Thi-5) had been equipped with composite piping to a large degree to mitigate corrosion issues and save weight, see Figure 6.

Figure 5. New and depleted iron anodes from the stainless steel filter indicating oxygen ingress in Sønderborg.

Figure 6. Composite piping installed in the new Thisted injector, Thi-5.

2.2 Mill scale sampling Sønderborg

Mill scale had been observed in new tubing of the type 9 5/8” (still mounted with end caps) at the Sønderborg site, Figure 1. This is not uncommon, and neither is the lifting of the mill scale as a result of undesirable storage conditions prior to installation (Figure 7), ref 28. However, when used for geothermal wells, mill scale should be completely removed. The ISO 11960 standard for tubing (ref 29) and the equivalent API 5CT standard do not include such requirements, so it should be specified specifically to have the mill scale removed. It is believed that this mill scale is released into the system in the installed wells, contributing to the experienced difficulties with injection. This is strongly supported by two reports on particles collected in the injection well, ref 10 and ref 15.

A sample of the scale was easily removed from the tubing as a result of poor adhesion to the surface, and its density estimated, by calculation of volume and the measured weight, to 1196.56 kg/m^3. With the 9 5/8" tubing making up the majority of the well, the release of mill scale would result in a released volume of 0.1 m^3/100 m tubing (62 kg/100 m) – enough to fill up 1.3 m of the injection well when assuming dense packing. Release of mill scale from the entire tubing length would make things even worse.

The XRD analysis in Appendix C shows heavy chloride contamination and calcium minerals, so perhaps the tubing has been exposed to the brine at some stage. Chloride contamination will promote the lifting/flaking of millscale considerably when exposed to humid atmosphere.

The previously conducted solubility test, by Added Values (ref 15), has been reproduced with the collected mill scale from Sønderborg. The test was carried out by attempting to dissolve 0.5 g of scale in 50 ml acid. Two acids were attempted; 2 % HF and 5 % HCl, at 50 °C. After 24 hours of exposure, the mill scale was largely unaffected, with only a minor fraction of the scale appearing to have dissolved. The observations coincide with the results obtained by Added Values, and it is equivalently our immediate conclusion that an acid job is unlikely to dissolve the released and sedimented mill scale.

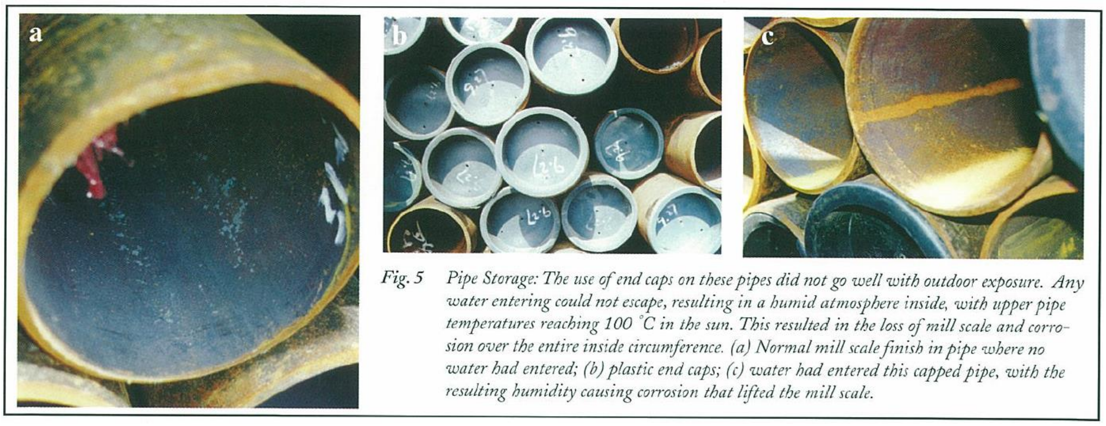

Fig. 5 *Pipe Storage: The use of end caps on these pipes did not go well with outdoor exposure. Any water entering could not escape, resulting in a humid atmosphere inside, with upper pipe temperatures reaching 100 °C in the sun. This resulted in the loss of mill scale and corrosion over the entire inside circumference. (a) Normal mill scale finish in pipe where no water had entered; (b) plastic end caps; (c) water had entered this capped pipe, with the resulting humidity causing corrosion that lifted the mill scale.*

Figure 7 Mill scale observed in steel piping showing the exact same characteristics as those observed for surplus tubing in Sønderborg. B. Dillon. Ref 28.

2.3 Corrosion measurements in Sønderborg 2017-2018

On-site monitoring with corrosion sensors took place just after the injection pump, as described earlier. A side-stream unit that could handle high pressure (up to 100 bar) had been constructed for this purpose, Figure 8. The measurements included exposure of coupons for the first half of 2017 and all three techniques for the entire heating season from November 2018 to April 2018.

The obtained results show large variations in the operating conditions, which is related to regular pressure build-up in the injection well, Figure 10. The corrosion rate measurements indicate ingress of air in the surface plant, possibly at the injection pump. This causes a relatively high corrosion rate of steel in the range of 0.1 to 0.3 mm/year, Table 2. Superficial pitting corrosion is also observed on the stainless steel coupons after exposure and cleaning, Figures 11 to 18. Since the corrosion rates were measured using three different techniques, there is a high degree of certainty in these results.

Figure 8. Side-stream unit for corrosion measurements in Sønderborg.

Figure 9. Automated water-sampler installed in Sønderborg.

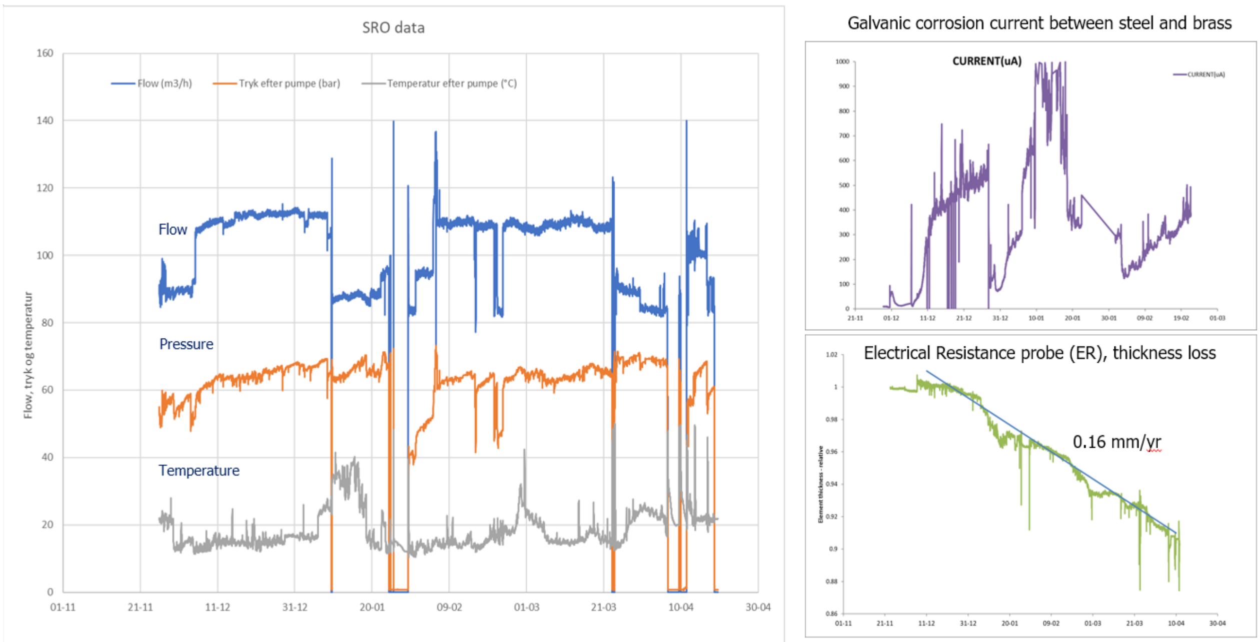

Figure 10 Results of on-line corrosion measurements in Sønderborg in the period from November 2017 to April 2018.

Figure 11. Steel coupon exposed for 5 months in Sønderborg loop after injection pump.

Figure 12. Stainless steel (316) exposed for 8 months in Sønderborg loop after injection pump.

Figure 13. Steel coupon after cleaning.

Figure 14. Stainless steel (316) coupon after cleaning.

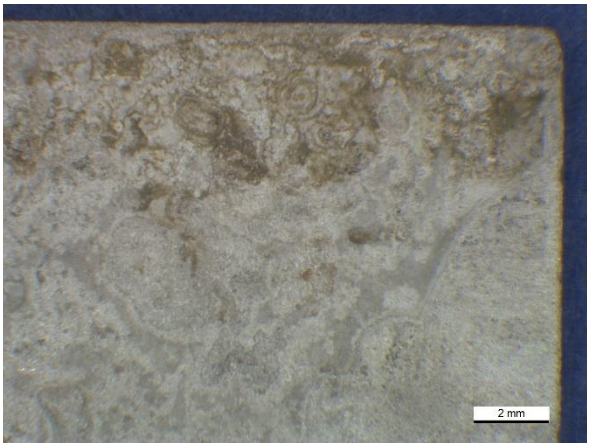

Figure 15. Close-up of uniform corrosion on steel coupon exposed for 5 months.

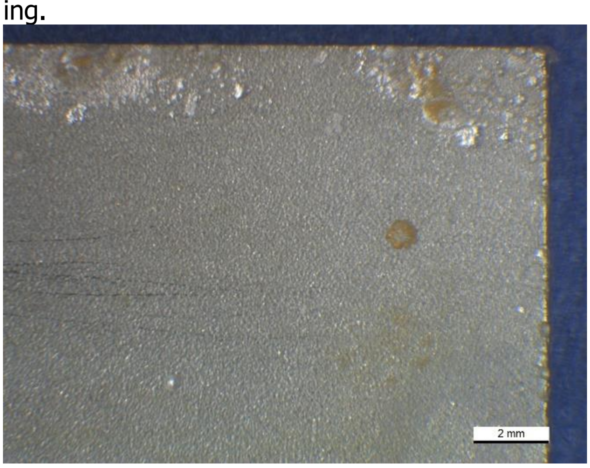

Figure 16. Close-up of pitting corrosion on stainless steel (316) exposed for 8 months.

Figure 17. Galvanic probe exposed for 5 months in Sønderborg loop after injection pump.

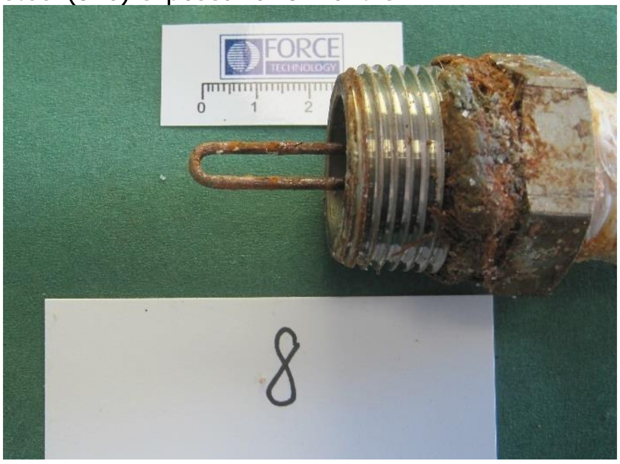

Figure 18. ER steel element exposed for 5 months in Sønderborg loop after injection pump.

Table 2. Results of corrosion monitoring in Sønderborg. Corrosion rates are calculated weight loss of the exposed coupons.

Pos.	Orientation	Material	Corrosion rate Feb2017–May2017 3 months' exposure mm/year	Corrosion rate Nov2017–Apr2018 5 months' exposure mm/year	Corrosion rate Both periods 8 months' exposure mm/year
1	In flow direction	C1018	0.099 *	0.21	
2	Opposite of flow	C1018	0.086 *	0.27	
3	In flow direction	C1018			0.33
4	Opposite of flow	C1018			0.36
5	In flow direction	316L			0.002
6	Opposite of flow	410 (13Cr)			(0.017)

*) * Sulphide scale, iodine azide positive.

The second campaign in Sønderborg started in December 2018, including on-line monitoring of pH, DO and ORP on both the production and the injection lines, Figure 9. Unfortunately, the plant was shut down unexpectedly after one week due to pressure build-up in the injection well.

The results obtained with the water sampling rack on the production line showed very stable pH (6.6-6.8) and an extremely low content of dissolved oxygen (~0.01 ppm), i.e. ideal conditions for preventing corrosion of steel, Figures 19 to 22.

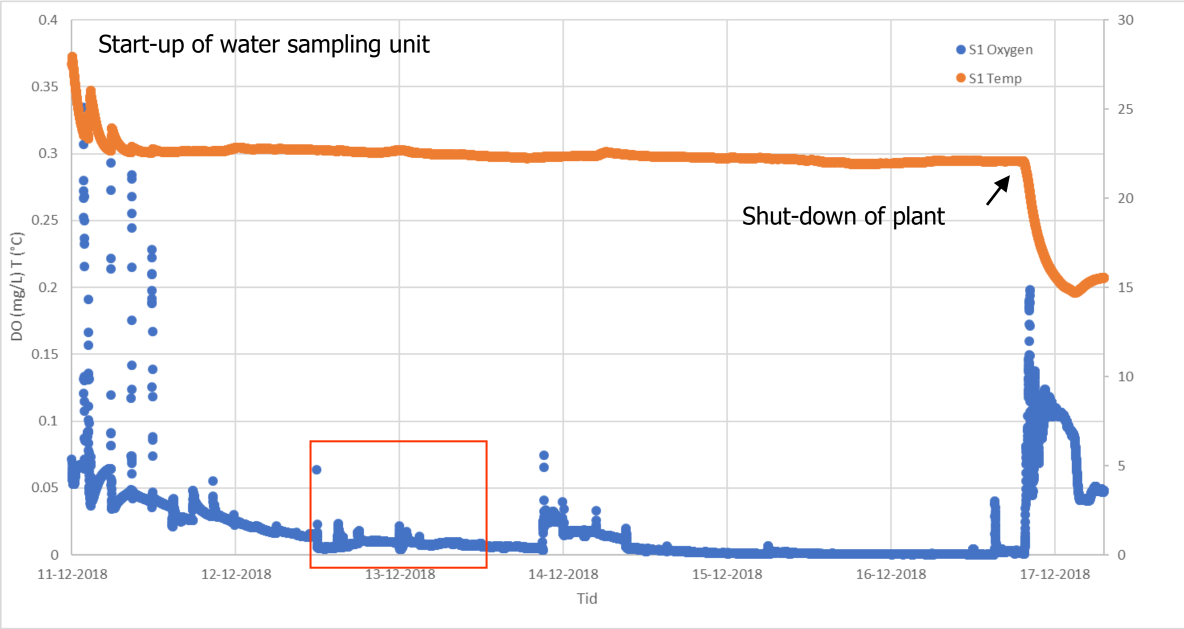

Figure 19 Results of dissolved oxygen measurement in Sønderborg in December 2018.

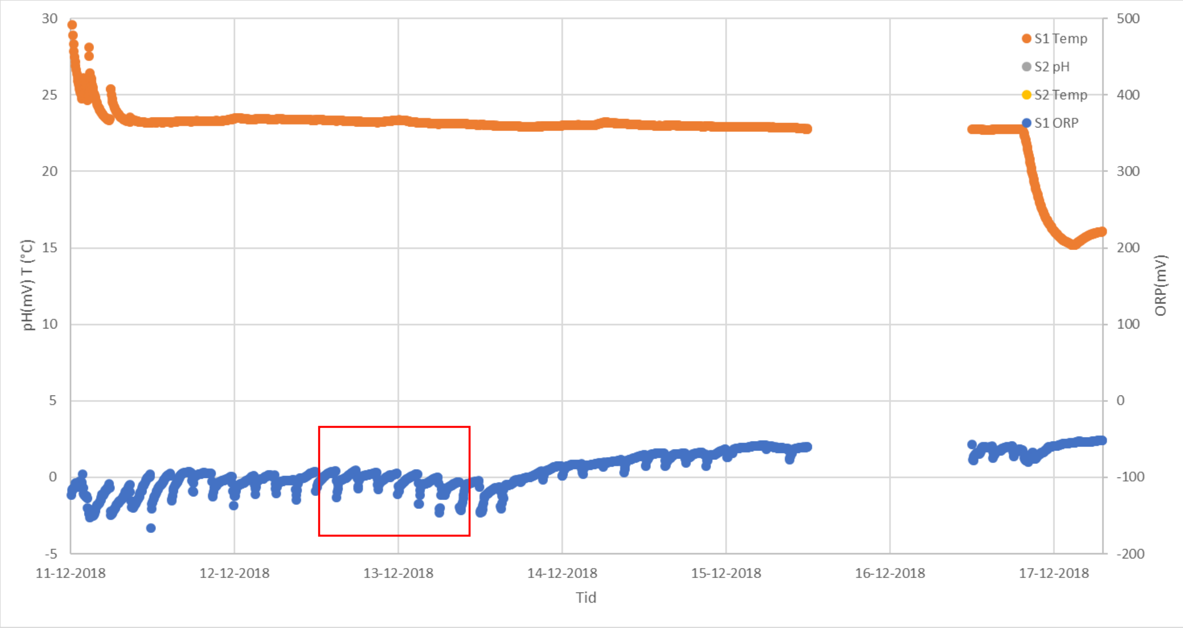

Figure 20 Results of pH and ORP measurements in Sønderborg in December 2019.

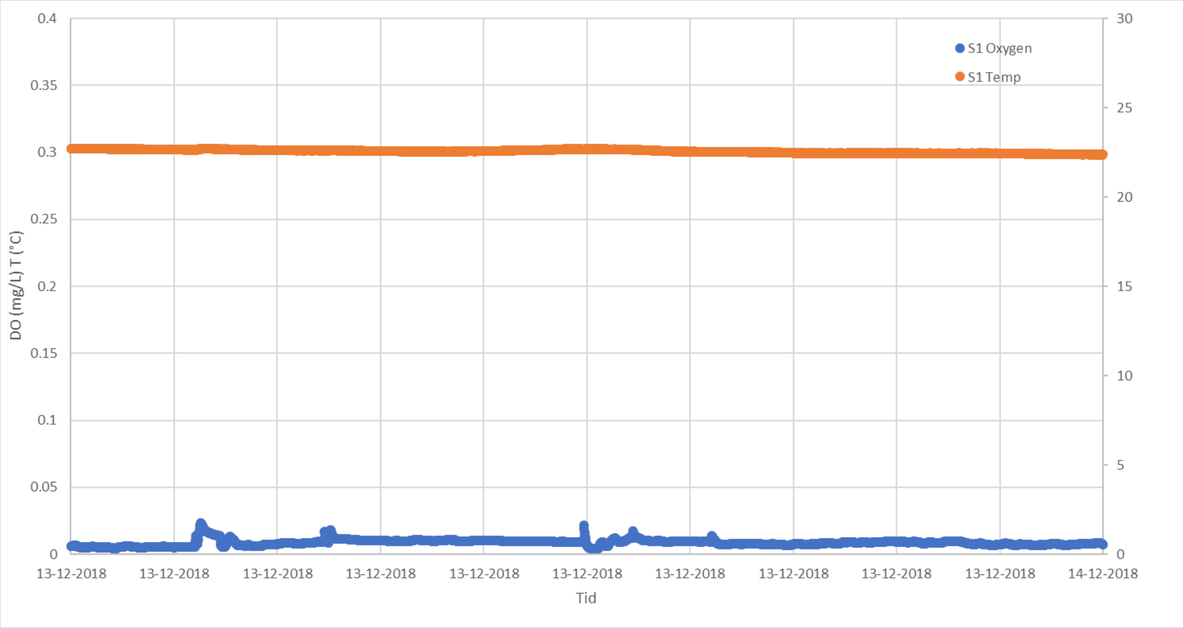

Figure 21 Close-up of dissolved oxygen measurements recorded over one day.

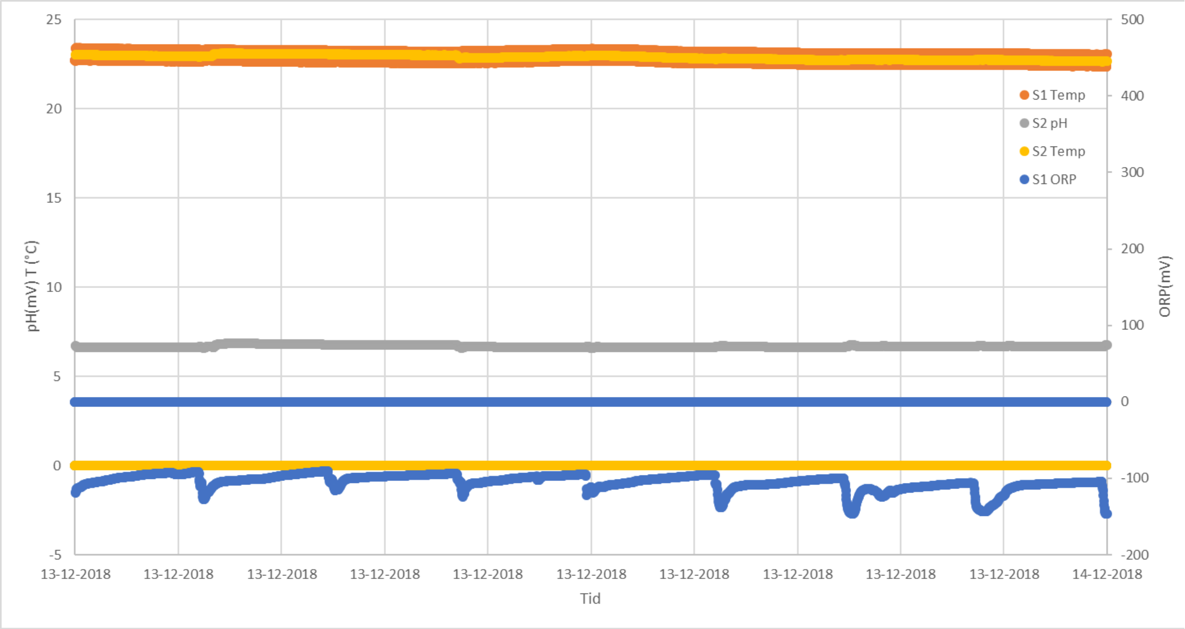

Figure 22 Close-up of pH and ORP measurements recorded over one day. A water sample is taken every 3rd hour for 5 minutes. This appears as spikes on the ORP curve.

2.4 Corrosion measurements at Margretheholm 2017

Due to problems with a leaking heat exchanger in the secondary circuit, the geothermal plant was shut down at the beginning of 2017. The leak and presence of NORM (Naturally Occurring Radioactive Material) in the piping and subsequent high costs associated with restarting the plant have caused the owner HOFOR to permanently shut down the plant. This unfortunately meant that no measurements were performed at Margretheholm with the new customised test setups. However, we managed to review some data from the Nalco sensors.

Due to problems with lead deposition, Nalco had installed a chemical dosage system and a corrosion monitoring rig at Margretheholm, Figure 23. The rig measures pH, oxidation reduction potential (ORP) and corrosion rate.

The data obtained during the first half of 2017 was reviewed and discussed with Nalco, Figure 24. Only a small part of the measurements is considered valid due to insufficient calibration or service of the probes.

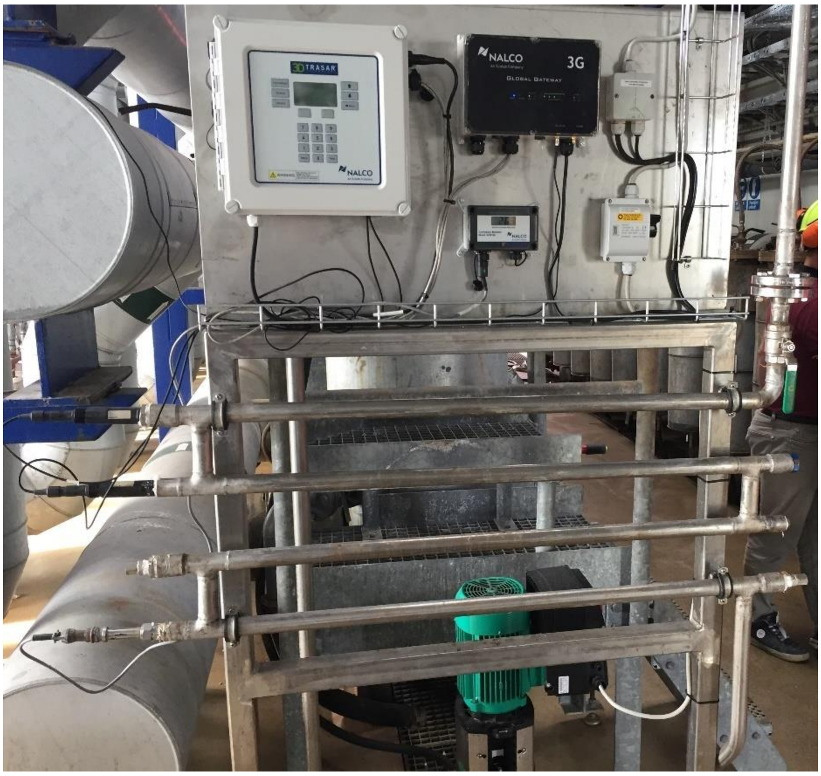

Figure 23. Setup for corrosion measurement at Margretheholm.

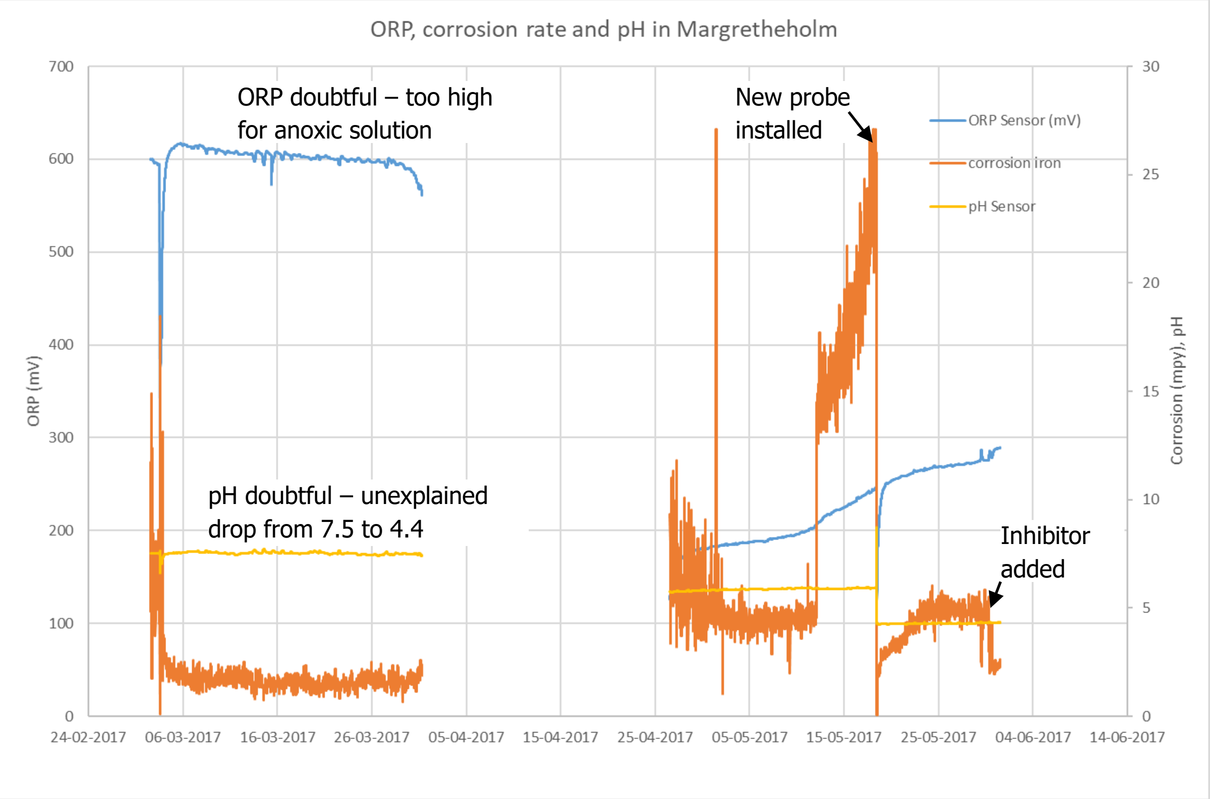

Figure 24. Corrosion monitoring data from measurements at Margretheholm 2017 after the filters.

An interesting part of the curve is when the corrosion inhibitor is added on 30 June 2017. Nalco GEO942 is added at a rate of 0.8 l/h to reach a concentration of 10 ppm. By this, the corrosion rate drops from 5 mpy (0.13 mm/year) to roughly 2.5 mpy (0.6 mm/year). The obtained effect of factor two is disappointing. Usually, a much higher inhibitor efficiency (> 90 %) is expected.

It should be noted that the corrosion rate measured with the applied technique is not exact. Typically, the measured rate can differ up to a factor 3 from the actual rate. However, the technique still provides valuable information about relative changes (e.g. inhibitor addition) or trends.

The measurements at Margretheholm demonstrate the complexity and need of constant follow-up when doing corrosion monitoring. The pH probe is quite sensitive and requires frequent calibration, and frequent check procedures should be applied to validate the measurements of e.g. the ORP and corrosion probes.

2.5 Water sampling in Thisted 2019

Although not originally in the test plan, one of the test racks was sent to Thisted to capture some data. One of the racks was mounted near the old injection well Thisted 3 on 26 March 2019, Figure 25. The rack was measuring for about one month before the plant was shut down for the summer on 25 April 2019.

The initial measurements showed some problems in obtaining stable readings during the 5-minute measurement period every 3rd hour, Figures 26 and 27. A possible cause of this is entrapment of gasses in the measurement cells for ORP/pH and DO. Small amounts of N_2 and CH_4 gas have previously been detected in the brine from the production well (ref 19). It was also difficult to control the flow; probably because of the relatively low inlet pressure. The flow control, including the control valve, should be reconsidered.

The best readings were obtained by establishing a constant flow through the cells for the remaining part of the test. For this period, the following observations were made:

- Dissolved oxygen (DO) is below the detection limit, i.e. in the ppb range.
- pH is very stable at 6.2.
- Oxidation reduction potential (ORP) is -80 mV vs Ag/AgCl.

The observed conditions are ideal to control corrosion of the steel tubing. This correlates well with the condition of the tube sample in Figure 2. Additionally, there are no signs of fluctuations in the service conditions of the plant.

The observed fluctuations, for especially the DO measurements, are related to limitations in design of the water sampling rack. Refinements may be made to obtain better readings, e.g. by adding a degasser. Also, a better data acquisition system is needed that is in sync with the sampling periods, when water flows through the cells. Operating the water sampler requires frequent supervision until the design and data handling have been improved.

Figure 25. Automated water sampler installed near the old injection well Thisted 3. It measures dissolved oxygen, pH and ORP in the water after cooling and depressurising.

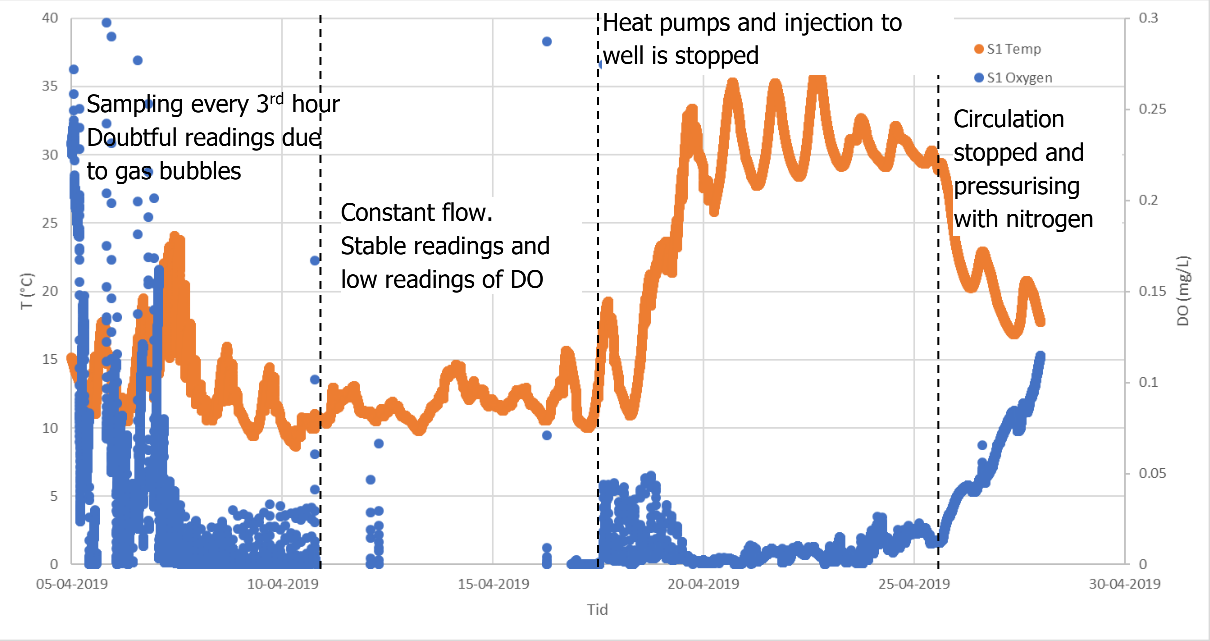

Figure 26. Result of dissolved oxygen measurements in Thisted. The temperature represents the water temperature in the measurement cell after cooling and depressurising.

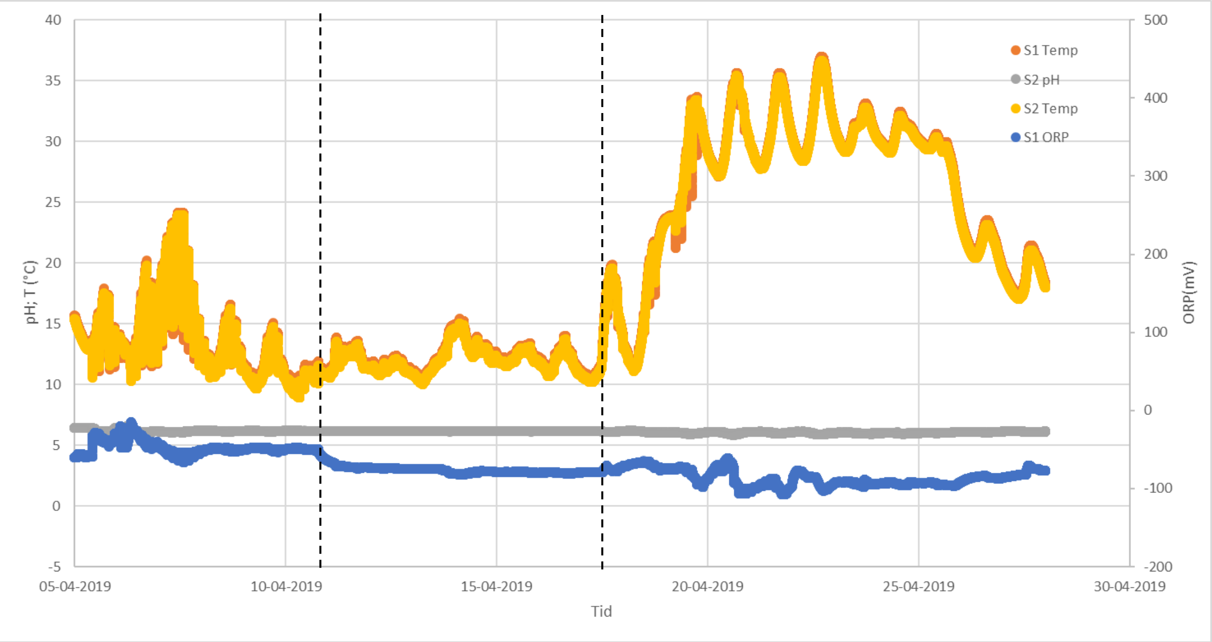

Figure 27. Result of pH and ORP measurements in Thisted. The temperature represents the water temperature in the measurement cells after cooling and depressurising.

3 Parametric laboratory testing

3.1 Oxygen, flow rate, temperature

Effects of basic parameters affecting corrosion have been examined in the laboratory at FORCE Technology using electrochemical techniques. The tests have been carried out in newly installed autoclaves as well as in traditional glassware setup.

Figure 28. Autoclave used for electrochemical testing in artificial brine solution.

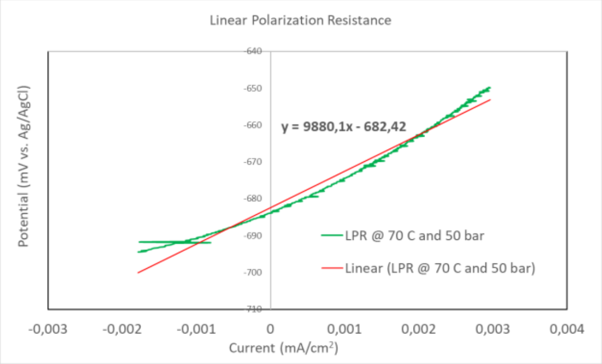

Area (cm^2)	4.41
Rest Potential (mV)	-685
Metal	Mild Steel
Metal factor	1159
LPR ($Ohm.cm^2$)	9880
Ba (mV/decade)	120
Bc (mV/decade)	120
Icorr (mA/cm^2)	0.00264
Corrosion Rate (mm/yearear)	0.031

Figure 29. Obtained LPR curve and assumptions for calculating the corrosion rate.

The first series of corrosion tests on steel was carried out in artificial Margretheholm brine solution. The corrosion behaviour is obtained by measuring the polarisation resistance (LPR) and corrosion potential with time. As mentioned earlier, the obtained corrosion rate based on LPR is indicative (within a factor 3) but the observed trends are reliable.

The measurements show a large effect of dissolved gas (oxygen or oxygen-depleted) and only moderate effects of stirring and temperature. The corrosion rate is not affected by the total pressure, Figure 30 and Table 3.

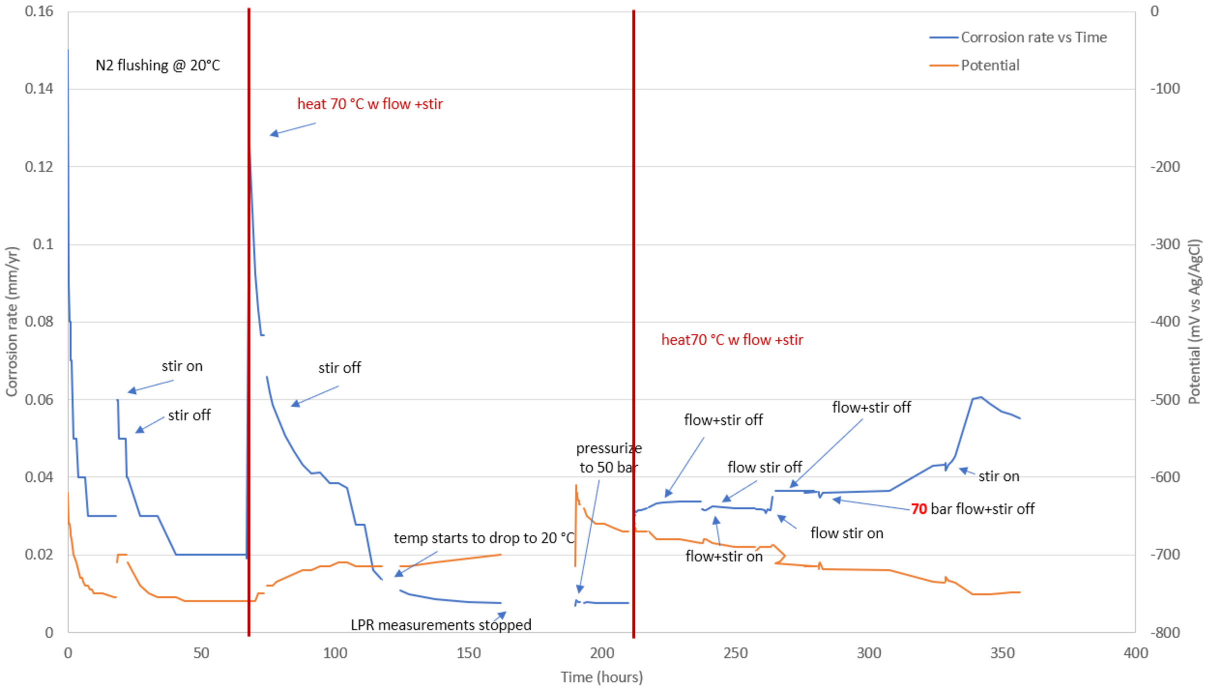

Figure 30. Corrosion behaviour of steel in artificial Margretheholm brine solution characterised by corrosion rate from LPR and corrosion potential.

Table 3. Results of parametric testing in artificial brine solution. Corrosion rates are measured with LPR in autoclave.

Gas	Temp.	Pressure	Stir	Corrosion rate (mm/year)
Air	20 °C	1 bar	No	0.15
N_2	20 °C	1 bar	No	0.01
N_2	20 °C	50 bar	No	0.01
N_2	70 °C	50 bar	No	0.03
N_2	70 °C	70 bar	No	0.03
N_2	70 °C	70 bar	Yes	0.06

3.2 Lead deposition

The effect of lead in solution and its deposition on the steel in artificial Margretheholm brine solution has been investigated using electrochemical techniques, such as LPR, open circuit potential (OCP), cyclic polarisation, and zero resistance amperometry (ZRA) on a galvanic coupling between steel and steel with lead in the brine solution. The steel with lead in solution represents virgin steel tubing exposed to the brine or newly exposed areas of old tubing from under newly removed deposits.

ZRA on coupling between steel and steel with lead added in solution showed a rapid response in the corrosion current upon the addition of lead to one of the electrodes at 25 and 70 °C, corresponding to corrosion rates of, respectively, 0.012 and 0.029 mm/year. This indicates that the kinetics allow rapid reduction of the Pb(II) to Pb, depositing the lead and corroding the steel as a result of the cathode and anode reaction:

$$Pb^{2+}\ 2e^{-} \rightarrow Pb \qquad \text{(cathode)}$$
$$Fe \rightarrow Fe^{2+} + 2e^{-} \qquad \text{(anode)}$$

However, slow normalisation of the current followed, indicating that the deposition process slows down as lead is being deposited and that the local galvanic cell on the steel with lead directly deposited is a slowly stabilising system.

Testing at 25 and 70 °C showed great influence of temperature on the kinetics of the deposition of lead and on the corrosion rate, as seen from Figure 31, with the effect being larger with increased temperature.

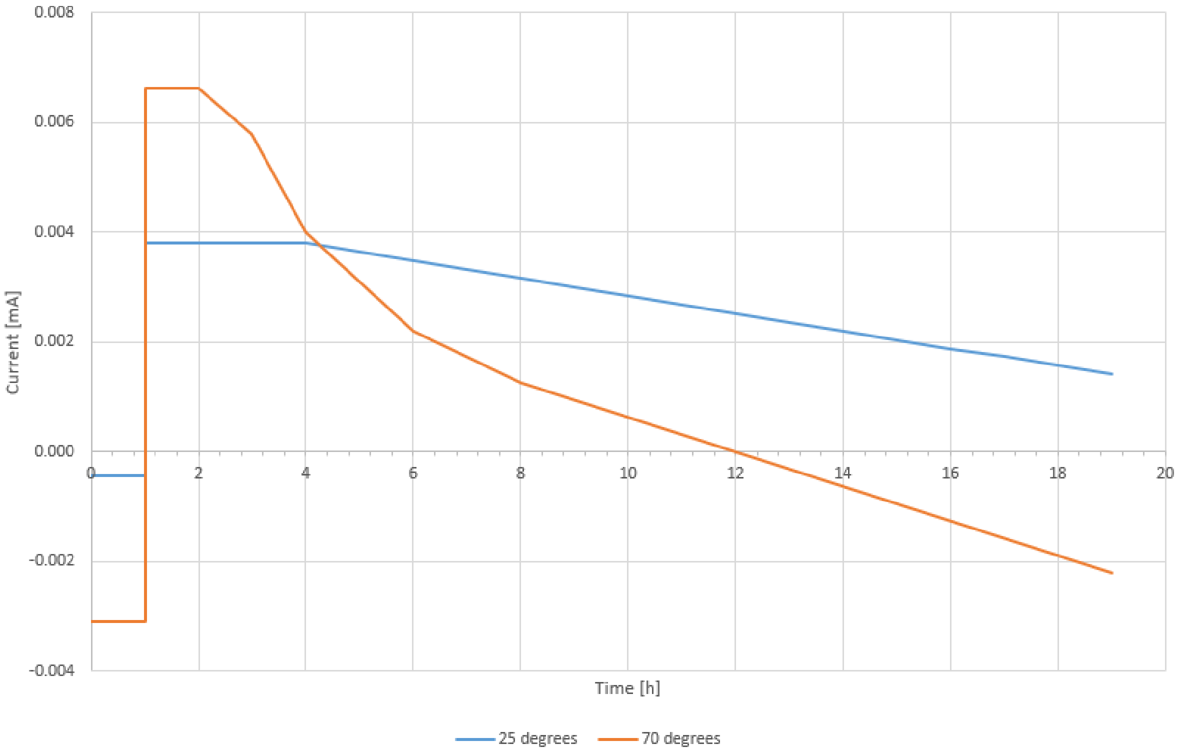

Figure 31. Galvanic corrosion current measurement (ZRA) for steel coupled to steel w. 3.0 mg/l Pb^{2+}. Showing the current measured over time between the two cells at 25 and 70 °C with N_2 flushing and stirring.

Cyclic polarisation was conducted on metallic lead, steel, and steel with lead added in solution prior to polarisation, again at 25 and 70 °C. In this case, lead is included to investigate the behaviour of already existing lead deposits and their effect on exposed adjacent steel.

Figures 32 and 33 depict the results showing the full steel curve (anodic and cathodic) and the cathodic curves of lead and steel with lead depositing from solution. Steel by itself corrodes faster in the artificial Margretheholm brine solution at 70 °C compared to the same at 25 °C, but with little change in corrosion potential. This is seen by the slight decrease in corrosion potential and the faster increase in running current with the rise in potential.

Steel with added lead in solution shows an increase in the corrosion potential and appears to have a great decrease in corrosion rate with temperature (see Table 4). This behaviour is still under investigation.

Lead on its own shows a decrease in corrosion potential but no change in corrosion rate with increased temperature. At this point, the high corrosion current of lead and accompanying corrosion rate are not explained; however, kinetics may play a role as well as may deposition of salt of Ca and Mg on the surface (ref 30) and the dissolution of natural lead oxide on the surface while initially being run as cathode during the test.

However, the lead or steel with lead depositing plotted as cathode reaction and steel as anode, as if they were coupled in the same system, show around a quarter decade increase in the corrosion current of the steel, and thus increased corrosion (see Table 4). The effect of temperature is therefore still evident, in accordance with the result of the ZRA measurements.

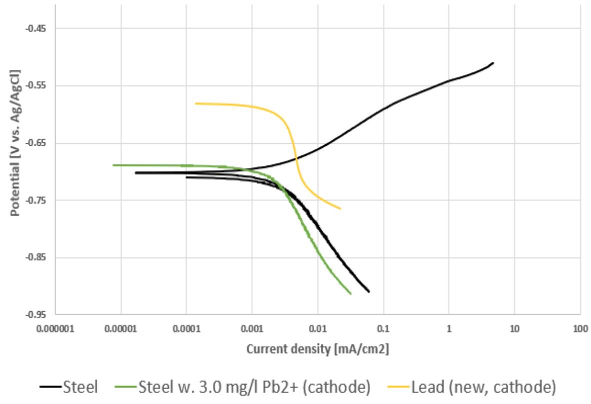

Figure 32. Cyclic polarisation in artificial brine at 25 °C with N_2 flushing and stirring.

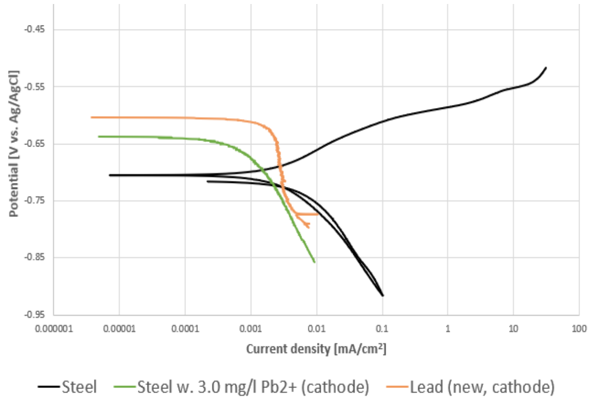

Figure 33. Cyclic polarisation in artificial brine at 70 °C with N_2 flushing and stirring.

A significant increase in corrosion rate of steel will occur if coupled to metallic lead in form of deposits, as is shown below in Table 4 for the steel/lead coupling. The opposite effect is indicated to occur during the process of lead deposition, when looking at the result of the cyclic polarisation. However, this contradicts the result from ZRA measurements where a current was indeed recorded (indicating increased corrosion), but the calculated corrosion rates are similar for the two methods.

Additionally, the effect of the Nalco corrosion inhibitor used at Margretheholm has been investigated showing more than a factor five reduction in corrosion rate with both 1 ppm and 10 ppm at 25 °C, with the polarisation curves illustrated in Figure 34. We have been informed by Hofor that the intended dosage level was 1 or 10 ppm. Similar reduction in corrosion rate at 25 °C was recorded using LPR with and without lead in solution, giving a reduction of a factor two and three.

At 70 °C, 1 ppm Nalco in solution yielded a factor two reduction in corrosion rate; however, 10 ppm unexpectedly showed an increase in corrosion rate although a more than 100 mV increase in corrosion potential was expected.

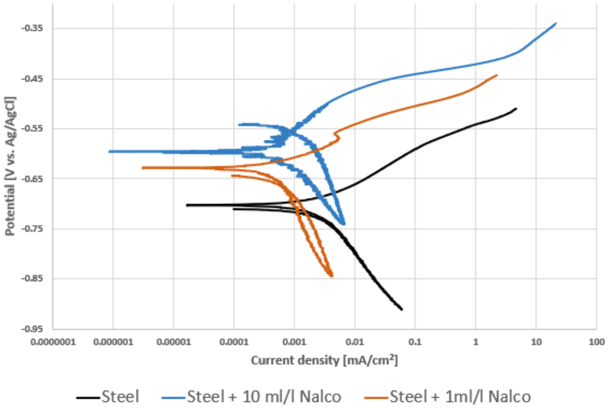

Figure 34. Cyclic polarisation in artificial brine at 25 °C with N_2 flushing and stirring.

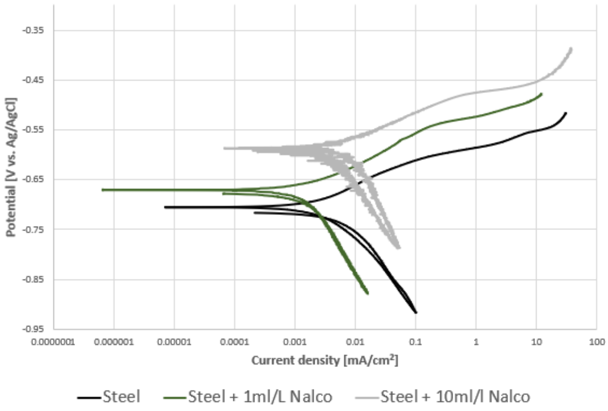

Figure 35. Cyclic polarisation in artificial brine at 70 °C with N_2 flushing and stirring.

Table 4. Corrosion rates calculated from cyclic polarisation, i.e. Tafel approximation on individual material polarisations curves (*based on theoretical coupling as illustrated in Figures 32 and 33).

Material	Temp.	Electrolyte	E_{corr} [mV]	Corrosion rate [mm/yr]
Steel St52	25 °C	Brine	-702	0.023
Steel St52	70 °C	Brine	-702	0.023
Steel St52	25 °C	Brine + 3.0 mg/l Pb^{2+}	-696	0.024
Steel St52	70 °C	Brine + 3.0 mg/l Pb^{2+}	-638	0.008
Steel St52	25 °C	Brine + 1 ml/l NALCO	-626	0.004
Steel St52	25 °C	Brine + 10 ml/l NALCO	-598	0.004
Steel St52	70 °C	Brine + 1 ml/l NALCO	-663	0.004
Steel St52	70 °C	Brine + 10 ml/l NALCO	-588	0.01
Lead	25 °C	Brine	-578	0.04
Lead	70 °C	Brine	-599	0.04
Steel/Steel w. 3.0 mg/l Pb^{2+}*	25 °C	Brine	-	0.009
Steel/Steel w. 3.0 mg/l Pb^{2+}*	70 °C	Brine	-	0.019
Steel/Lead*	25 °C	Brine	-	0.058
Steel/Lead*	70 °C	Brine	-	0.035

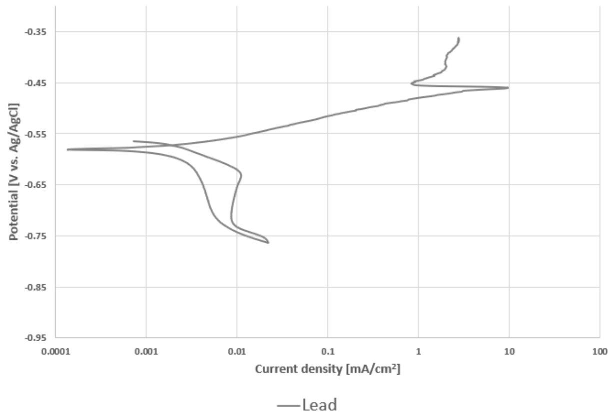

Figure 36. Cyclic polarisation of lead in artificial brine at 25 °C with N_2 flushing and stirring.

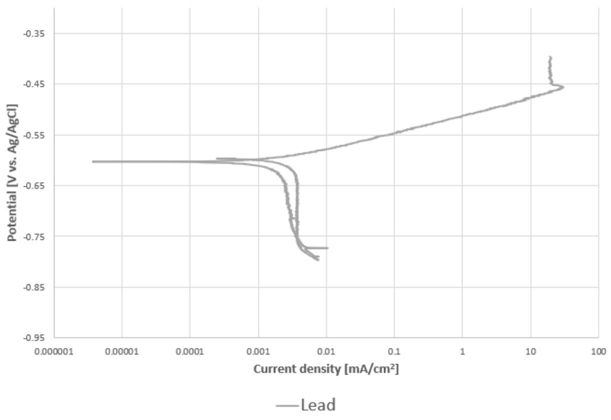

Figure 37. Cyclic polarisation of lead in artificial brine at 70 °C with N_2 flushing and stirring.

Pure lead was tested to obtain information about the corrosion behaviour of a metallic lead coating formed in the geothermal plant, Table 5 and Figures 36-37. Lead has higher corrosion rate when compared with steel, but at the same time lead is more electropositive or noble, i.e. the corrosion potential is higher. Lead seems to passivate at potentials above -0.45 V Ag/AgCl. This is seen especially at 25 °C, where the current drops one decade.

3.3 Corrosion resistant alloys

As it has been seen for cyclic polarisation of St52, also stainless steel 316L appears to benefit from the presence of lead in solution. Passive stainless steel will behave as cathode and lead as anode in many conditions, and with the recorded OCP for lead and stainless steel 316L, this is found also to be the case in the artificial brine.

Table 5. Pitting (E_{pit}) and repassivation (E_{rp}) potentials obtained from cyclic potentiodynamic polarisation for 316L in artificial brine at 25 °C and 70 °C.

Material	Temp.	Electrolyte	OCP [mV]	E_{pit} [mV] at 10 μA/cm^2	E_{rp} [mV] at 1 μA/cm^2
Stainless Steel 316 L	25 °C	Brine	-27	251	-81
Stainless Steel 316 L	70 °C	Brine	-166	-62	-269
Stainless Steel 316 L	25 °C	Brine + 3.0 mg/l Pb^{2+}	-8	216	-59
Stainless Steel 316 L	70 °C	Brine + 3.0 mg/l Pb^{2+}	-56	7	-268

As cyclic potentiodynamic polarisations measurements (shown below in Figures 38 and 39, and summarised in Table 5) depict, at 25 °C the lead reduces the pitting potential (E_{pit}) of 316L making it more susceptible to localised corrosion initiating. In terms of repassivation potential (E_{rp}), lead does not appear to have a significant effect at either 25 °C or 70 °C. However, at 70 °C, the pitting potential of 316L increases and passive current is lower with the presence of lead in solution. This may be due to rapid deposition of a thin layer of lead on the surface as a result of the higher temperature. Therefore, it is possible that lead either adsorbs to the passive film on the stainless steel or it forms a substance with poor solubility, e.g. lead oxide or lead sulphide.

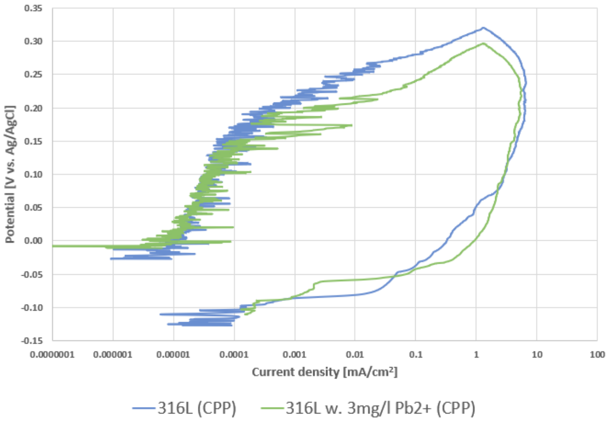

Figure 38. Cyclic potentiodynamic polarisation in artificial brine at 25 °C with N_2 flushing and stirring.

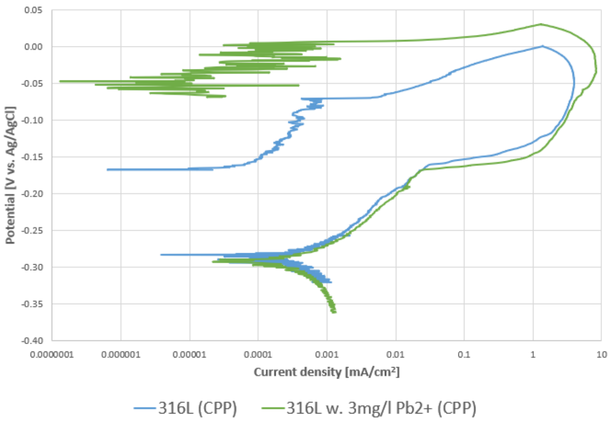

Figure 39. Cyclic potentiodynamic polarisation in artificial brine at 70 °C with N_2 flushing and stirring.

4 Discussion and conclusions

The experimental work in WP5 has been focused on the mechanisms that could release particles in the injection well due to corrosion. The specific conditions for the Danish geothermal plants have been covered, having steel as the main construction material.

At Margretheholm, deposition of lead that causes galvanic corrosion of steel may contribute considerably to reduced injectivity. Literature on electrochemical corrosion of lead in salt brines is scarce, so a major part of the laboratory testing has focused on developing test methods. Lead is more noble than steel, which explains galvanic dissolution of steel, but less obvious effects are also seen, especially the temperature dependence and behaviour of stainless steel. The dosage of corrosion inhibitor has only limited effect (2-5 times) as shown in the on-site measurements and laboratory testing.

Apart from lead in the brine, ingress of oxygen presents a great risk of corrosion of both steel and stainless steel. In Sønderborg, quite high corrosion rates of steel are observed at the injection well, using the side-stream corrosion rack. Several independent test methods were used and all point to oxygen ingress as the main reason for corrosion. Unfortunately, the simultaneous measurement of dissolved oxygen could not be performed as intended. However, the measurements at the production well in Sønderborg and at the injection well in Thisted show that very low oxygen content is attainable. This is underlined by the pipe sample from Thisted, showing no corrosion after 30 years' service.

Stainless steel type AISI 316L has also been tested. As expected, the tolerance to corrosion in the high-saline brine is very low, especially in hot brine. It basically depends on the residual oxygen content that should be kept below 20 ppb (according to standards in the oil and gas industry). No damage has been reported for the AISI 316L stainless steel parts in the plants today. This is because all parts are in contact with carbon steel or iron anodes. However, upgrading entire pipe systems and well tubing to stainless steel is not yet viable unless ingress of oxygen can be controlled better.

On this basis, additional efforts are still needed to identify the exact cause of the oxygen ingress at the plant in Sønderborg. The injection pump and start/stop operations are suspected as the main sources, but measurements are needed to prove it - as soon as the plant becomes operational again. Here, experience gained from operating the customised equipment for on-site corrosion monitoring and water sampling will benefit any future campaigns.

The observed mill scale on the inside surface of surplus well tubing is an important finding in the project. The mill scale can cause considerable release of rust flakes that might plug the injection well. This could already be seen after one year's service in Sønderborg, and most likely, the oxygen ingress has promoted the release of rust flakes. Testing has shown that mill scale is extremely difficult to dissolve, making a well workover impossible. The acids needed to dissolve mill scale would possibly damage both reservoir and well completion. Thus, the requirements for well tubing for geothermal energy should be stricter than those met in the oil and gas industry, where tubing having mill scale is often installed. The leading standards for well tubing (API 5CT and DS/EN ISO 11960) do not address mill scale and surface quality requirements at all.

5 Suggestions to future work

The joint efforts in WP5 have brought many new interesting observations, as highlighted in Executive summary. However, we still see a need for future work to deal with corrosion, scaling and microbiology in aggressive brines.

- Mill scale on the inside surface of well tubing should be studied further. It may be a completely neglected issue in the geothermal energy sector and the tubing standards don't address it. Test should be made to assess whether mill scale is released in the installed tubing operating under deaerated conditions - or is it only a problem in tubing stored on the ground in highly aerated conditions? Camera inspections of the injection well in Sønderborg may show this.

- The results obtained with corrosion inhibitors for lead and galvanic corrosion show only little improvement. Continued testing is recommended to identify more efficient corrosion inhibitors if the operation of Margretheholm resumes.

- Reason for beneficial effect of lead on corrosion resistance of stainless steel in hot brine should be identified.

- Definitive documentation of the possible oxygen ingress in the Sønderborg should be made when the plant resumes service.

- Refinements should be made to the automated water-sampler to improve flow control, de-gassing and data logging features. The stainless steel tray and tubing should be replaced with corrosion resistant polymer materials or coatings in the open drain system.

- Test and qualification of airtight gaskets and solutions for the surface plant, including composite piping where oxygen permeation might be a problem.

- Impact of standstill periods on microbiological growth should be measured.

6 References

1. Joachim Tremosa, Nicolas Marty, Vincent Bouchot, Experience with geothermal plants in France, BRGM, July 2017.
2. Mikael Erlström, The Lund Geothermal System Background, design and review of operational experiences, Lund University, 27. June 2017.
3. Nicole Pastrik and Andrea Förster, GEOTHERM – Geothermal energy from sedimentary reservoirs – Removing obstacles for large scale utilization, GFZ German Research Centre for Geosciences, 30. June 2017.
4. Assessment of Scale and Possible Corrosion Due to the Presence of Lead in Produced Water in a Geothermal Well, IFE Report, 2015-12-14.
5. Blypartikler i posefiltre på GDA skyldes muligvis midlertidige blyudfældninger i anlæg, GEUS notat, 14-08-2015.
6. MAH – IFE_Corrosion study – Executive summary, Petter Schanke, Ross DK, 14/12/2015
7. Årsag til injektionsproblemer i MAH-1A, vurderet ud fra partikelundersøgelser. GEUS document 08-EN-14-14.
8. Soft acidizing lab-experiments with microscope details, GEUS presentation June 20th 2017
9. Grain size curves for three Danish geothermal wells, GEUS, Presentation 2013.
10. Undersøgelser af injektionsboring ved geotermianlægget i Sønderborg, GEUS notat, 08-EN-14-10, 23.juni 2014.
11. Assessment of Corrosion in Sønderborg Geothermal Wells, IFE Report, 2016-02-17.
12. Sønderborg – IFE_Corrosion study – Executive summary, Petter Schanke, Ross DK, 03/03/2016.
13. Mitigation of the corrosion and deposition problems at the Sønderborg geothermal plant, CFG Services, 21/04/2016.
14. Undersøgelse af prøvemateriale fra injektionsboring ved geotermi anlægget i Sønderborg, Added Values rapport, 17. juli 2014.
15. Vurdering af mulighed for kemisk rensning af injektionsboring ved Sønderborg geotermianlæg, Added Values rapport, 15. august 2014.
16. Partikler i geotermivand, membran filterprøver udtaget 25-26 febr. 2015 i Sønderborg, GEUS notat, 21. marts 2015.
17. Mikrobiel sulfiddannelse i Sønderborgs geotermiske anlæg, GEUS notat, 25. februar 2016.
18. Membranfilterprøver viser zinksulfid og blysulfid i Sønderborg geotermiske anlæg, GEUS notat, 2015.
19. Thisted suspended solids and formation water chemistry December 2015, GEUS notat, 27-04-2016.
20. Lead deposition in geothermal installations, TNO 2014 R11416, P.M.M.C. Bressers & F. Wilschut, 2014.
21. Minutes of WP5.2 meeting, 2017-06-15.
22. www.geothermaleranet.is/media/publications-2015/Geothermal-ERA-NET-JA-Report-OpERA_publication_def_MC_Update_20161010.pdf.
23. H. Schröder et al, Long term reliability of geothermal plants – Examples from Germany, Proceedings European Geothermal Congress 2007, Unterhaching, Germany, 30 May-1 June 2007.
24. Lead in formation water causes problems in geothermal exploitation, GEUS rapport, 15-10-2015.

25. Nye undersøgelser indikerer at partikelindholdet i injektionsvandet øges når køling ikke fungerer, GEUS rapport, 16-02-2015.
26. Partikler i injektionsvand i injektionsvand membran filterprøver udtaget 16. februar 2015 på GDA, GEUS rapport, 16-02-2015.
27. Partikler i injektionsvand membran filterprøver udtaget 14. januar 2015 på GDA, GEUS rapport, 14-01-2015.
28. Barry Dillon, Transit Damage and Hot Rolled Steel, Practical Failure Analysis, Volume 2(4) August 2002.
29. DS/EN ISO 11960:2014, Petroleum and natural gas industries -- Steel pipes for use as casing or tubing for wells.
30. Metals Handbook, 9th edition, Volume 13 – Corrosion, Corrosion of Lead and Lead Alloys, 1987.

Appendix A.

	Margretheholm	Sønderborg	Thisted	Reference
Reservoir Rock				
Formation and age	Bunter Sandstone Fm	Gassum Fm	Gassum Fm	*Margretheholm:* Mathiesen, A. (2008) *Sønderborg:* Vosgerau et al. (2015A) *Thisted:* Hjuler et al. (2014)
Depositional environment	Fluvial/aeolian	Shoreface/fluviatile	Estuarine	*Margretheholm:* *Sønderborg:* *Thisted:* Hjuler et al. (2014)
Burial history, depth, temperature and pressure (see below for temp.)	Basinal deposits/ 2400 m Hydrostatic press.	Basinal deposits/ 1100 m Hydrostatic press.	Basinal deposits/ 1200 m Hydrostatic press.	*Margretheholm:* *Sønderborg:* Vosgerau et al. (2015A) *Thisted:* Hjuler et al. (2014)
Lithology (including a lithological log of the reservoir)	Sandstone	Sandstone	Sandstone	*Margretheholm:* Mathiesen, A. (2008) *Sønderborg:* Vosgerau et al. (2015A) *Thisted:* Hjuler et al. (2014) Vosgerau et al. (2015B)
Net/Gross and gross sand	0.35 / 137m	0.97 / 40m	0.74 / 95m	*Margretheholm:* GEUS (interne data) *Sønderborg:* Vosgerau et al. (2015A) *Thisted:* Vosgerau et al. (2015B)
Porosity and permeability	20% / 400mD	28% / 3500mD	25% / 1600mD	*Margretheholm:* GEUS (interne data) *Sønderborg:* Vosgerau et al. (2015A) *Thisted:* Vosgerau et al. (2015B)
Mineralogical composition	Quartz + Feldspar	Quartz + Feldspar	Quartz + Feldspar	GEUS
Geothermal plant				
Age of the plant in operation	12 years	4 years	33 years	*Margretheholm:* Mahler & Magtengaard (2005) *Sønderborg:* Vosgerau et al. (2015A) *Thisted:* Vosgerau et al. (2015B)
Distance in reservoir between production and injection wells	1.3 Km	600 m	1.5 Km	*Margretheholm:* Mahler & Magtengaard (2005) *Sønderborg:* Vosgerau et al. (2015A) *Thisted:* Hjuler et al. (2014)
Pipeline materials	Carbon steel piping with 5 mm corrosion allowance		Carbon steel piping, 3 mm corrosion allowance	*Margretheholm:* Mahler & Magtengaard (2005) *Sønderborg:* *Thisted: Røgen et al. (2015)*

Appendix A.

Corrosion	One case of through-wall corrosion in line after heat-exchanger	No	One case of external corrosion on topside pipe.	
Monitoring of corrosion or scaling	Yes	Yes	No	

Reservoir and production data

Reservoir temperature, surface temperature and injection temperature	73°C / 8°C (actually 15-25°C)	48°C / 8°C (actually 15-20°C)	TH-2 44°C / 8-15°C	*Margretheholm:* Mathiesen, A. (2008) *Sønderborg:* Vosgerau et al. (2015A) *Thisted:* Vosgerau et al. (2015B)
Reservoir pressure, plant operating pressure and injection pressure	1.03-1,04 SG EMW, 10–15 bar, 50-70 bar well head pressure	1.03-1,04 SG EMW, 10–15 bar, 50-70 bar well head pressure	1.03-1,04 SG EMW, 10–15 bar, 26-27 bar well head pressure	*Margretheholm:* Mahler & Magtengaard (2005) *Sønderborg: DONG Sønderborg FWR (2010)* *Thisted: Søren H.Damgaard, Driftschef*
Salt concentration and influence on production performance	TDS: 218 g/l Na-Ca-Cl	TDS: 164 g/l Na-Ca-Cl	TDS: 167 g/l Na-Ca-Cl	*Margretheholm:* Mahler & Magtengaard (2005) *Sønderborg:* Vosgerau et al. (2015A) *Thisted:* Vosgerau et al. (2015B)
Flow rate(s), seasonal variations	Max 235 m^3/h	Max 350 m^3/h (actual 70-80 m^3/h)	Actual 170 m^3/h	*Margretheholm:* Mahler & Magtengaard (2005) *Sønderborg: DONG Sønderborg FWR (2010)* *Thisted: Søren H.Damgaard, Driftschef*
Annual hours of operations	-	-	5000 hours	
Average annual heat production	-	-	24000 MWh	
Actual plant performance versus designed yield	-	-		Thisted: afgiftsstyret pga. affaldsforbrænding

Appendix A.

Well design

Casing design details including materials	**MAH-1** 30” conductor (H-40, 457 lb/ft) 13 3/8” (K-55, 54.4 lb/ft) 9 5/8” liner (K-55, 40 lb/ft) 9 5/8” tubing (L-80, 47 lb/ft) **MAH-2** 30” conductor 13 3/8” K55 68 lb/ft 9 5/8” (K-55, 40 lb/ft)	**SG-1** 30” conductor 18 5/8” K55 87.5ppf 15” L80 92.5 lb/ft x 13 3/8” K55 68ppf 9 5/8 L80 47ppf 9 5/8“ (53.5 lb/ft) 9 5/8 (K-55, 40 lb/ft) **SG-2** 30” conductor (456 lb/ft) 18 5/8” (K-55, 87.5 lb/ft) 15” (L-80, 92.5 lb/ft) 13 3/8” (K-55, 68 lb/ft) 9 5/8”	**Thisted-2** 30“ conductor (K-55) 18 5/8“ (C-75) 13 3/8“ (N-80) 9 5/8“ (N-80) **Thisted-3** 20“ (K-55) 13 3/8“ (K-55) 9 5/8“ (N-80) 7“ sand blasted tubing	*Margretheholm:* MAH-1 and MAH-2 completion reports *Thisted:* Thisted 2 and 3 completion reports Se ny tegning
Filter type and dimension	Perforated 9 5/8” liner K55 40 lb/ft,	7" Bakerweld Screen (6 gauge), 7" 29 lb/ft TS3 SB Box x Pin, 0.0062 slots	6.063” screen .012” slots	*Thisted:* Completion Program – Thisted-2 and -3, October 1984
Reservoir completion details	Perforated 9 5/8” liner K55 40ppf,	40/60 mesh gravel pack sand	20/40 mesh gravel pack sand	
Production completion, tubing, ESP (Electric Submersible Pump), etc.	9 5/8 K55 40ppf, SLB ESP type ???	9 5/8 K55 40ppf, SLB ESP type ???		
Wellhead configuration	DrilQuip 2k geothermal well head	DrilQuip 2k geothermal well head		
Operational performance				
Optimal day-to-day operation of the plant (including explanations on any chemical injections and precautions during start-up/shot-down)				
Downtime due to:				
- Loss of injectivity/reservoir completion plugging	Yes	Yes	No	
- Workover due to ESP replacement, frequency and duration			ESP exchanged October 2014. Pull: 2 days. Run: 3 days.	

Appendix A.

- Workover/intervention – scale and/or corrosion issues.				
- Well Integrity investigation		Gas leak at 13 378" x 15"	No	DFG and Ross leak investigation reports 2015
- Caliper corrosion log, frequency and duration	Performed but not processed 2015	No	No	
- NORM precipitation/deposition	Yes	No	No	
- Salt precipitation	Pb deposits from electrochemical reaction	No	No	GEUS report August 2015.
Laboratory tests performed to support the understanding of scaling problems (other than analysis of particles/scale and water samples)				

References

Hjuler, M.L., Vosgerau, H., Nielsen, C.M, Frykman, P., Kristensen, L., Mathiesen, A., Bidstrup, T. & Nielsen, L.H. 2014: Assessment of potential capacity increase of the existing geothermal plant at Thisted by adding a new geothermal well. *Danmarks og Grønlands Geologiske Undersøgelse Rapport*, **2013/80**, 90 pp.

Mahler, A. & Magtengaard, J. (2010): Country Update Report for Denmark. *Proceedings World Geothermal Congress 2010*, Bali, Indonesia, 25-29 April 2010.

Røgen, B., Ditlefsen, C., Vankilde-Petersen, T., Nielsen, L.H., Mahler, A. (2015) Geothermal Energy Use, 2015 Country Update for Denmark, *Proceedings Wordls Geothermal Congress 2015*, Melbourne, Australia, 19-25 April 2015.

Mathiesen, A. (2008): Varmen fra Jordens indre. *Aktuel Naturvidenskab*, **6**, pp. 18–20.

Vosgerau, H., Mathiesen, A., Kristensen L., Andersen, M.S., Hjuler, M.L. & Laier, T. 2015A: Det geotermiske screeningsprojekt. Sønderborg-lokaliteten. Det geotermiske screeningsprojekt: Energipolitisk aftale af 22. marts 2012. *Danmarks og Grønlands Geologiske Undersøgelse Rapport*, **2015/33**, 30 pp.

Vosgerau, H., Mathiesen, A., Kristensen L., Andersen, M.S., Hjuler, M.L. & Laier, T. 2015B: Det geotermiske screeningsprojekt. Thisted-lokaliteten. Det geotermiske screeningsprojekt: Energipolitisk aftale af 22. marts 2012. *Danmarks og Grønlands Geologiske Undersøgelse Rapport*, **2015/47**, 31pp.

GEUS report August 2015: Blypartikler i posefiltre på GDA skyldes muligvis midlertidige blyudfældninger i anlæg

Appendix A.

Thisted-2

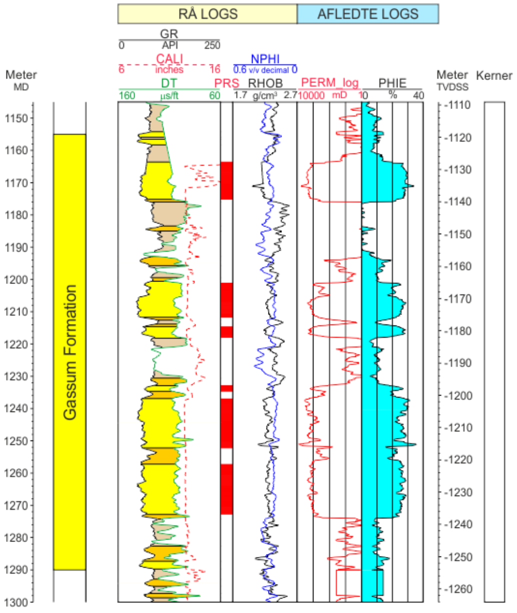

GR	Gamma-log
Cali	Caliper-log
DT	Sonic-log
PRS	Potentielt reservoirsand
NPHI	Total porøsitetslog
RHOB	Densitetslog
PERM_log	Permeabilitetslog
PHIE	Effektiv porøsitetslog
MD	Målt dybde
TVDSS	Total vertikal dybde under havniveau

🟨 Sandsten

🟧 Siltsten

🟫 Lerskifer

🟥 Potentielt reservoirsand

Thisted-3

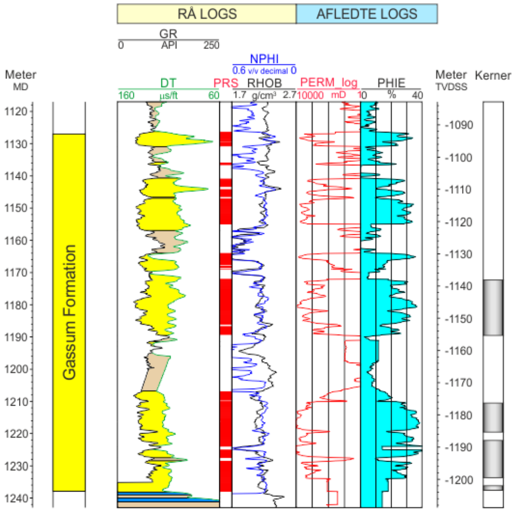

GR	Gamma-log
Cali	Caliper-log
DT	Sonic-log
PRS	Potentielt reservoirsand
NPHI	Total porøsitetslog
RHOB	Densitetslog
PERM_log	Permeabilitetslog
PHIE	Effektiv porøsitetslog
MD	Målt dybde
TVDSS	Total vertikal dybde under havniveau

🟨 Sandsten

🟫 Lerskifer

🟦 Kalksten

🟥 Potentielt reservoirsand

Appendix A.

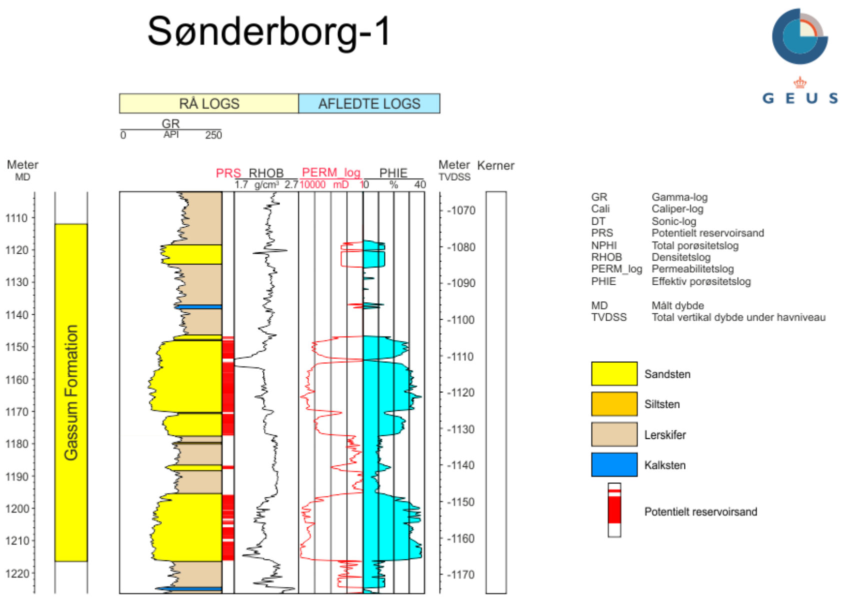

GR	Gamma-log
Cali	Caliper-log
DT	Sonic-log
PRS	Potentielt reservoirsand
NPHI	Total porøsitetslog
RHOB	Densitetslog
PERM_log	Permeabilitetslog
PHIE	Effektiv porøsitetslog
MD	Målt dybde
TVDSS	Total vertikal dybde under havniveau

🟨 Sandsten
🟧 Siltsten
▨ Lerskifer
🟦 Kalksten
🟥 Potentielt reservoirsand

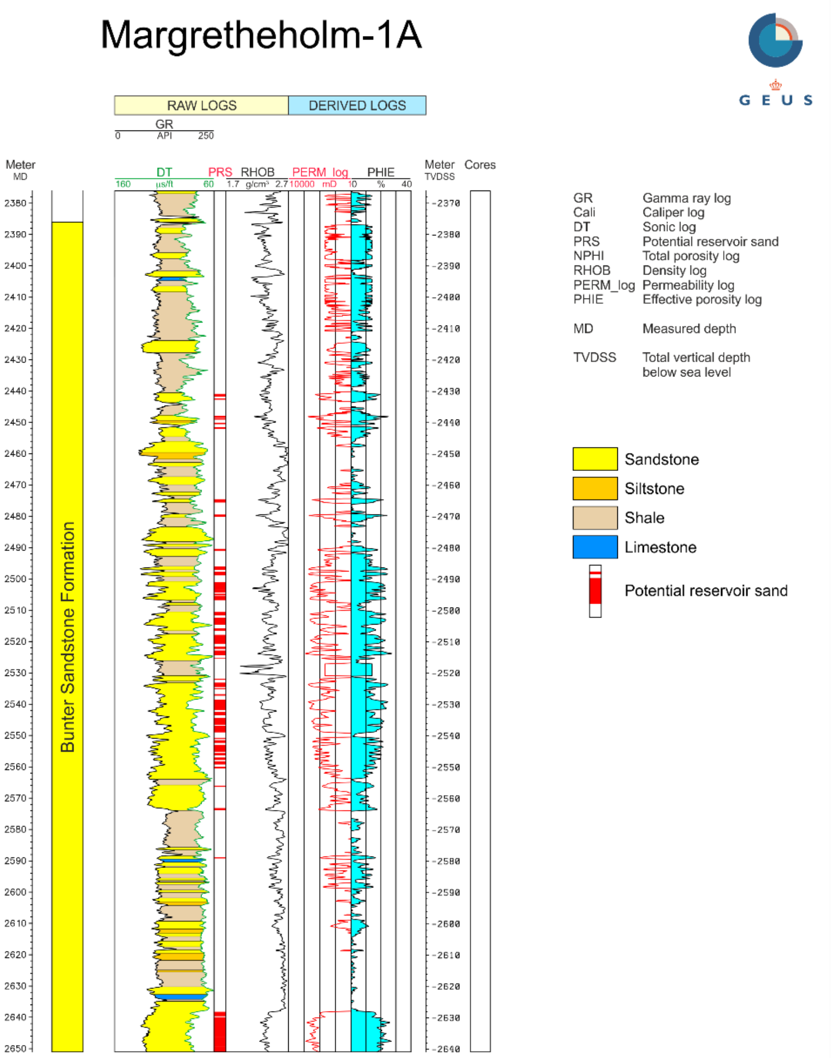

GR	Gamma ray log
Cali	Caliper log
DT	Sonic log
PRS	Potential reservoir sand
NPHI	Total porosity log
RHOB	Density log
PERM_log	Permeability log
PHIE	Effective porosity log
MD	Measured depth
TVDSS	Total vertical depth below sea level

🟨 Sandstone
🟧 Siltstone
▨ Shale
🟦 Limestone
🟥 Potential reservoir sand

Appendix B Composition of brine samples from Danish geothermal plants

			Margretheholm - Production well									
	A	B	C	A	A	C	A	C	A			
Chemical analysis of formation water from Margrtheholm geothemal wells												
Well	MAH-2	MAH-2	MAH-2	MAH-2	MAH-2	MAH-2	MAH-2	MAH-2	MAH-2			
Sample	Well Head	Filter1 72C	Injekt 20C	Well Head	Well Head	Injector	Well Head	Injector 20C	Well Head			
Lab	GEUS	GEUS	GEUS	GEUS	GEUS	GEUS	GEUS	GEUS	GEUS			
Date	16-07-2003	16-02-2015	16-02-2015	01-06-2016	04-06-2016	04-06-2016	03-03-2017	03-03-2017	17-03-2017			
Time	10:30 AM	10:30 AM	11:15 AM	12:30 PM	12:00 PM	1:45 PM	8:00 AM	8:15 AM				
pH	6.20	6.8	6.8				6.32	6.28	5.56			
Element/ion	mg/L	mg/L	mg/L									
Hydrogen Carb.	47	48	54				28.6	30.6	29.7			
Chloride, Cl	135400	134800	134600	133000			143500	142600	133963			
Bromide, Br	820	860	740	600			1040	1150	814			
Iodide, I	1.4	n.a.	n.a.									
Sulphate, SO4	284	375	369	210			220	230	230			
Sodium, Na	53500	52800	51300	54900	55000	54900	54100	53800	53974			
Calcium, Ca	23500	22200	23600	20900	20800	20900	20300	20400	20505			
Magnesium, Mg	2720	2820	2770	2950	2890	2890	2820	3020	2938			
Strontium, Sr	944	822	876	804	744	721	780	780	724.85			
Potassium, K	750	1160	1190	630	610	620	600	550	636			
Iron (tot.), Fe	4.6	1.8	2.4	5.1	6.9	3.9	17.4	15.1	0			
Manganese, Mn	25	26.3	27.8	17.6	15.8	15.5	20.1	19.2	16.75			
Ammonium, NH4	n.a.	n.a.	n.a.									
Zinc, Zn	6	3.8	4.3	2.6	2.3	2.1	3.8	3.9	3.67			
Barium, Ba	5.5	9	9.1	21.2	20.7	20	19.6	19.7	17.28			
Lithium, Li	11.8	14	13.9	10.2	8.3	8.3	10.8	10.6	9.67			
Lead, Pb	0.4	0.38	0.36	4.09	0.52	0.22	0.75	0.38	0.55			
Nickel, Ni		0.09	0.1	0.13	0.16	0.16	0.27	0.25	0.00			
Copper, Cu	0.4	0.06	0.07	0.07	0.06	0.06	0.44	0.36	0.0			
Silicium, Si									5.58			
Filter1= warm water after filter-bags, Filter2= cold water after second set of filters. n.a. = not analyzed												
Gas:water ratio	c. 0.11			0.11					0.692	0.692	0.116	0.116
Gas composition	vol%	vol%	vol%	vol%					vol%			
Ar	n.a.	0.6										
O2	*	<0.1	*						*	*	*	*
He	n.a.	n.a.	n.a.									
N2	84	89.5	80						91	93	93	92
CO2	3.6	0.4	1.4						1.6	0.6	0.8	1.0
CH4	13	6.7	9.4						7.4	6.3	6.3	6.9
H2	n.a.	n.a.	n.a.									
C2H6	140 ppm	n.a.	n.a.									
C3H8	7 ppm	n.a.	n.a.									
C4H10	2 ppm	n.a.	n.a.									
Note: * calculated O2-free												

Margretheholm - Injection well

Sampling location	D	E	E	D
Chemical analysis of formation water from Margrtheholm geothemal wells				
Well	MAH-1	MAH-1	MAH-1	MAH-1
Sample	Well Head	downhole sample/2480 m		Well Head
Lab	GEUS	BWG	BWG	GEUS
Date	03-08-2002	04-08-2002	04-08-2002	17-03-2017
Time	6:30 AM	9:30 AM	1:30 PM	
pH	6.55	6.05	6.05	5.73
Element/ion	mg/L	mg/L	mg/L	
Hydrogen Carb.	33	60	55	30
Chloride, Cl	137000	132000	133000	132877
Bromide, Br	870	790	750	879
Iodide, I	1.6	7.2	7	
Sulphate, SO4	240	272	282	222
Sodium, Na	53650	52900	54000	53864
Calcium, Ca	23480	23000	23100	20483
Magnesium, Mg	2910	2760	2550	2914
Strontium, Sr	905	860	870	705.91
Potassium, K	690	650	650	667
Iron (tot.), Fe	0	9.4	6.5	0
Manganese, Mn	27	15.1	13.1	17.11
Ammonium, NH4	n.a.	20.5	20.5	
Zinc, Zn	7	5.7	4.7	2.63
Barium, Ba	5.8	8.3	3.8	15.64
Lithium, Li	13	7.5	7.5	9.78
Lead, Pb	0.3	n.a.	n.a.	0.01
Nickel, Ni				0.00
Copper, Cu	0.3	n.a.	n.a.	0.00
Silicium, Si				5.73

Filter1= warm water after filter-bags, Filter2= cold water after second set of filters. n.a. = not analyzed

Gas:water ratio		0.147	0.14
Gas composition		vol%	vol%
Ar		~0.5	~0.5
O2		*	*
He		1.3	1.7
N2		84	88
CO2		7	7
CH4		7	3
H2		<0.1	<0.1
C2H6		<220 ppm	<90 ppm
C3H8		<220 ppm	<90 ppm
C4H10		<220 ppm	<90 ppm

Note: * calculated O2-free

Sønderborg produktionsboring

Chemical analysis of water samples from SG-1A, first pump test

Sampling location: A

Sample	Date	Kl.	pH	HCO3	Cl	Br	SO4	Na	K	Mg	Ca	Fe2+	Mn	Sr	Zn	Ba	Pb
type				---------------- mg/l ----------------				------------------------------ mg/l ----------------------------------									
formationsvand	25-06-2010	23:55	6.5	102	98000	350	900	53000	450	1150	4400	11					
formationsvand	26-06-2010	00:50	6.5	103	97000	350	900	53000	440	1150	4400	11					
formationsvand	26-06-2010	01:45	6.6	100	97000	350	900	53000	400	1150	4400	10					
formationsvand	26-06-2010	02:45	6.5	96	97000	350	900	53000	400	1150	4420	11					
formationsvand	26-06-2010	03:30	6.5	102	97000	350	900	53000	380	1150	4420	10	7	180	0.7	0.5	0.02

Chemical analysis of water analysis before and after cooling

Sampling location

Prøve	Date	Temp	pH	HCO3	Cl	Br	SO4	Na	K	Mg	Ca	Fe2+	Mn	Sr	Zn	Ba	Pb	
type		°C		---------------- mg/l ----------------				------------------------------ mg/l ----------------------------------										
formationsvand	04-12-2015	48	6.5	100	98500	340	810	54200	190	1170	4600	19	6	220	0.06	0.7	0.03	A
formationsvand	04-12-2015	15	6.5	96	99000	310	760	55900	190	1180	4600	20	6	220	0.08	0.7	0.02	B

Sample	Date	Temp	pH	HCO3	Cl	Br	SO4	Na	K	Mg	Ca	Fe2+	Mn	Sr	Zn	Ba	Pb	Si	
type		°C		---------------- mg/l ----------------				------------------------------ mg/l ----------------------------------											
formationsvand	22-03-2017	46	6.24	60	97149	219	729	55249	219	1101	3898.95	6	6	193	0.14	0.8	0.01	5.65	A
Well Head	22-03-2017	15.9	6.53	62	96228	222	737	55443	218	1093	3918	12	6	198	0.51	0.7	0.006	4.60	B

Gascontent in formation water from SG-2

Sample type	Date	Gas:Liquid ratio (mL:L)	Temp	$Ar+O_2$	H_2	N_2	CO_2	CH_4
Gas-liuid equilibrium at 1 bar	04-12-2015	17	48	1.5	3	93	2.2	0.05
Gas-liuid equilibrium at 1 bar	22-03-2017	8	46	-	-	98	1.7	0.22
Gas-liuid equilibrium at 1 bar	22-03-2017	8	46	-	-	97	2.1	0.42

Sønderborg injection well

Chemical analysis of water samples from SG-1A, first pump test

Pumpning the well clean of drilling mud. The first samples are influenced by drilling mud noticable by the high K content

Sample location C

Sample	Date	Kl.	pH	HCO3	Cl	Br	SO4	Na	K	Mg	Ca	Fe2+
type				---------------- mg/l -------------				------------------------- mg/l ----------------				
Completion fluid	17-05-2010	23:15	8.6	314	182000	700	117	84600	56100	75	100	1
formationsvand	18-05-2010	00:15	6.7	126	101000	500	900	56200	3960	1170	3520	17
formationsvand	18-05-2010	01:20	6.8	109	99000	400	900	54500	1020	1210	4200	18
formationsvand	18-05-2010	02:20	6.8	106	96000	320	900	52200	670	1220	4410	17
formationsvand	18-05-2010	03:40	6.6	106	96000	320	900	52300	620	1210	4430	18
formationsvand	18-05-2010	05:20	6.6	94	96000	320	910	52700	330	1210	4430	15
formationsvand	18-05-2010	06:20	6.7	100	96000	320	910	52400	330	1210	4400	17

Chemical analysis of the bottom hole samples from SG-1A

No pumping fromthe well since the first pump test

Sample location: D

Sample	Date	Kl.	pH	HCO3	Cl	Br	SO4	Na	K	Mg	Ca	Fe2+	Mn	Sr	Zn	Ba	Pb
type				--------------- mg/l ---------------				---------------------------- mg/l ---------------------------------									
Bottom Hole No. 1	24-06-2010		6.8	137	98050	187	820	54300	780	1130	4390	80	6	190	0.16	0.9	0.007
Bottom Hole No. 2	24-06-2010		6.8	102	99000	165	780	54500	800	1130	4410	82	6	200	0.16	0.9	0.007

Thisted

Chemical analysis of formation water from Thisted geothemal wells

Sampling location	A	A	B	A	B
Well	Thi-2	Thi-2	Thi-2	Prod. boring	Inj. boring
Sample	Well Head	Well Head	Aft. Cooling		
Date	18-01-1983	18-12-2015	18-12-2015	20-03-2017	20-03-2017
Temperature (°C)				43.2	15.6
pH	6.40	6.2	6.2	5.9	6.2
Element/ion	mg/L	mg/L	mg/L	mg/L	mg/L
Hydrogen Carb.	40	45	45	31	40
Chloride, Cl	102000	102000	103000	98642	98582
Bromide, Br	290	430	430	314	317
Sulphate, SO4	25	69	86	-	-
Sodium, Na	55000	55000	55000	51882	51914
Calcium, Ca	7500	7400	7500	6909	6881
Magnesium, Mg	1700	1500	1600	1564	1492
Strontium, Sr	360	350	340	370.04	388.21
Potassium, K	250	265	270	248	193
Iron (dissolved) Fe	36	30	29	8	19
Manganese, Mn	16	13	13	15	15
Zinc, Zn	0.6	0.09	0.12	1.0	0.05
Barium, Ba	12	13	13	18	17.55
Lead, Pb	0.04	0.02	0.02	0.01	0.00
Silicium, Si				4.65	4.93

Concentrations are in mg/L

	Thi-2 02-09-1984				Thi-2 20-03-2017		
Gas:water ratio	0.085	0.085	0.09		0.01	0.01	0.01
Gas composition	vol%	vol%	vol%		vol%	vol%	vol%
Ar	0.23	0.25	1		-	-	-
O2	0.15	0.2	*		-	-	-
He	0.7	0.6	n.a.		-	-	-
N2	37.9	37.9	42.3		52.9	56.5	51.0
CO2	2.1	1.9	2.0		1.2	1.7	1.9
CH4	57.5	57.7	54.2		45.8	41.8	47.1
H2	0.4	0.92	n.a.		-	-	-
C2H6	0.3	0.43	n.a.		-	-	-
C3H8	0.003	0.005	n.a.		-	-	-

Note: * calculated O2-free

Appendix C XRD and chemical analysis of products

XRD analysis of mill scale from tubing in Sønderborg

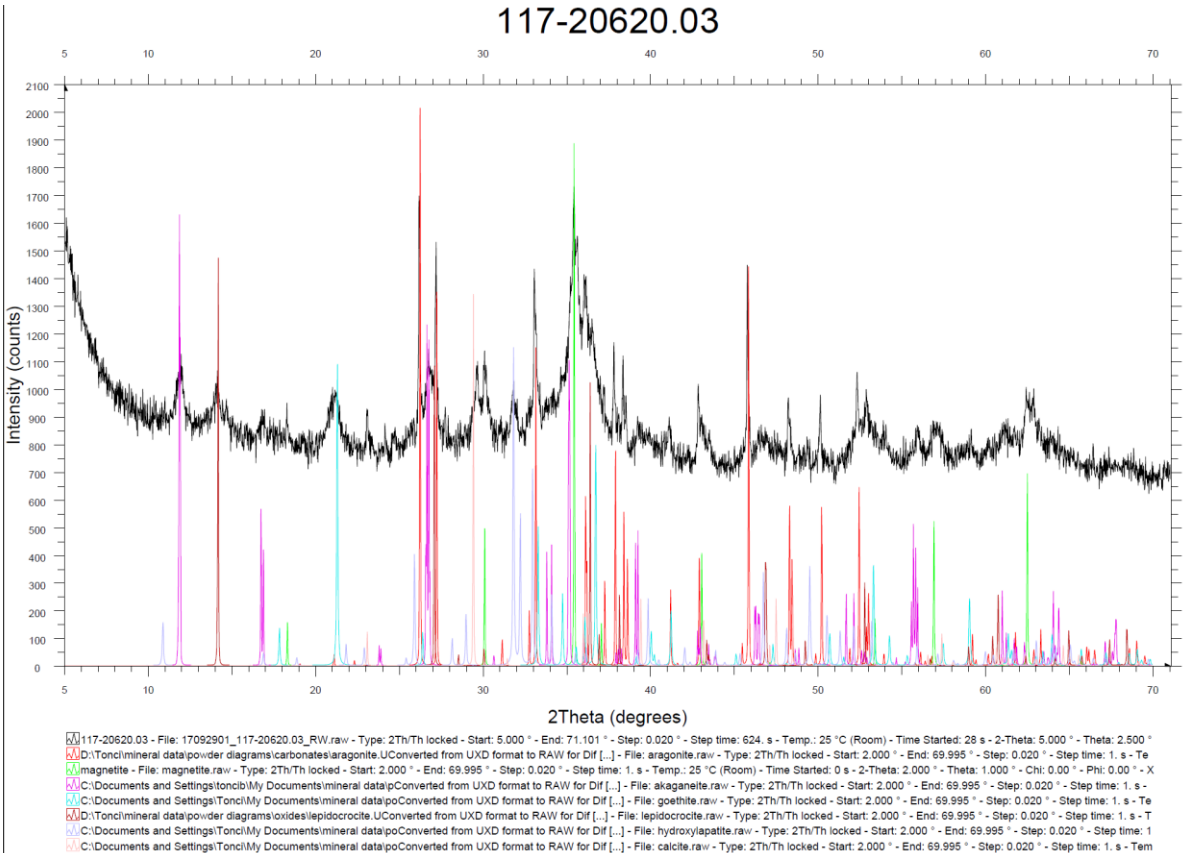

The mill scale contains

• Goethite	α-FeO(OH)
• Akaganiete	$FeO_{0.833}(OH)_{1.167}Cl_{0.167}$
• Lepidocrocite	γ-FeO(OH)
• Hydroxyapatite	$Ca_{10}(PO_4)_6(OH)_2$
• Aragonite	$CaCO_3$
• Calcite	$CaCO_3$

SEM analysis of products taken from a filterbag in Margretheholm

116-20421.20

Author:	pia
Creation:	09/26/2016 1:46:38 PM
Sample Name:	grå afsætning

Area 1

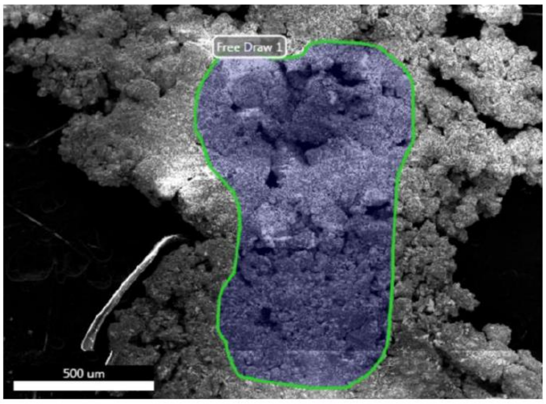

Notes:

Pia Hansen
2016-09-26

Digitally signed by Pia Hansen
pj@force.dk
Specialist

Karina Brotoft
2016-09-27

Digitally signed by Karina Brotoft
khu@force.dk
Technician

Free Draw 1

kV: 20 Mag: 64 Takeoff: 33.6 Live Time(s): 50 Amp Time(μs): 7.68 Resolution:(eV)

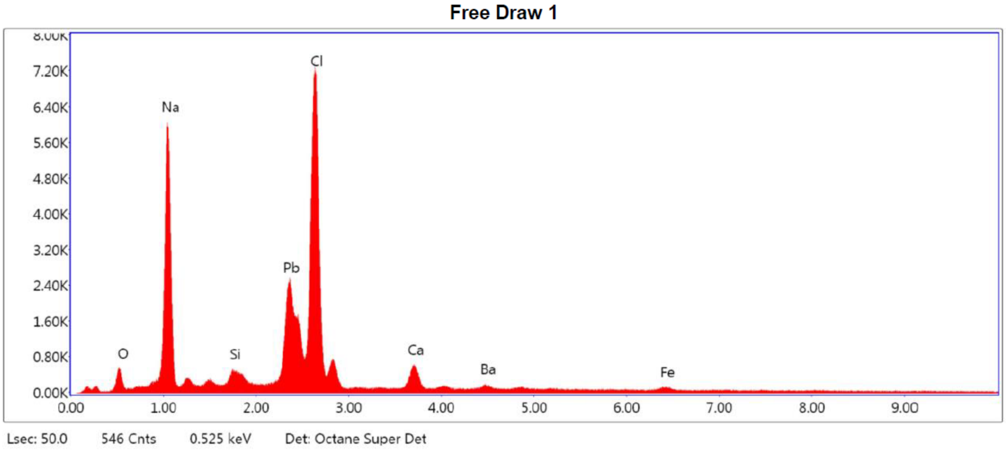

eZAF Smart Quant Results with SEC (07.07.2016)

Element	Weight %	Atomic %
O K	7.6	15.6
NaK	32.2	45.6
SiK	1.0	1.2
PbM	18.8	3.0
ClK	33.1	30.4
CaK	3.8	3.1
BaL	2.2	0.5
FeK	1.2	0.7